The Effects of Si and Humic Acid on U (VI) Removal from the Savannah River Site F/H Area groundwater

by Joel McGill, DOE Fellow
Dr. Yelena Katsenovich, Mentor
Applied Research Center

Background

Between 1955 and 1988, the F/H Area Seepage Basins located in the center of SRS received approximately 1.8 billion gallons of acidic waste solutions (pH from 3.2 to 5.5) contaminated with a variety of radionuclides and dissolved metals. The constituents of concern (COCs) associated with the F-Area groundwater plume are tritium, uranium-238, iodine-129, and strontium-90. The COCs in the H-Area are tritium, strontium-90 and mercury. A pump-and-treat water treatment unit was designed and built in 1997. Soon they switched to a re-injection system using a carbonate base. However it has been shown that alkaline carbon solutions can enhance the mobility of uranium and reverse the effects of natural adsorption.

Objective

- Investigate if dissolved sodium silicate solutions have enough alkalinity to replace the carbonate base used to correct the acidic nature of the contaminated sediments.
- Determine if there are any synergistic interactions between U(VI) ions, HA and Si:
  - Study the influence of Humic Acid (HA) and Si on the sorption of U(VI) onto F/H Area sediments.

Results

Sample-Description pH 4	U(VI) Avg. Removal, %	Std.	Si Avg. Removal, %	Std.	Fe, ppm
Filtered Batch 1	34.36	23.13	97.83	1.81	No soil
Batch 2	22.33	1.65	93.02	0.95	No soil
Batch 3	15.18	3.42	No Si	NA	No soil
Batch 4	57.71	7.5	97.89	0.75	0.1-0.2
Batch 5	87.36	8.81	93.55	3.36	0.2-1.3
Batch 6	78.1	1.34	No Si	NA	0.2-0.6
Batch 7	45.83	3.02	No Si	NA	0.1-0.3

Sample-Description pH 5	U(VI) Avg. Removal, %	Std.	Si Avg. Removal, %	Std.	Fe, ppm
Batch 1/ Filtered	81.88/ 92.80	1.98/0.76	94.09	0.92	No soil
Batch 2	29.65	19.55	62.76	13.17	No soil
Batch 3	9.29	5.43	No Si	NA	No soil
Batch 4	88.66	0.39	79.19	2.27	0.01-0.02
Batch 5	81.16	3.70	83.37	5.58	0.09-0.11
Batch 6	86.05	2.47	No Si	NA	0.19-0.24
Batch 7	88.81	3.34	No Si	NA	0.1

Sample-Description pH 6	U(VI) Avg. Removal, %	Std.	Si Avg. Removal, %	Std.	Fe, ppm
Batch 1/ Filtered	82.19/98.8	3.44/0.05	94.09 /96.21	0.92 /0.51	No soil
Batch 2	59.84	4.37	62.76	13.17	No soil
Batch 3	55.72	11.79	No Si	NA	No soil
Batch 4	92.62	4.3	79.19	2.27	0.013
Batch 5	92.10	2.28	83.37	5.58	0.66-0.84
Batch 6	94.53	0.05	No Si	NA	0.82-1.05
Batch 7	99.08	0.3	No Si	NA	0


Figure R-1: Batches 4-8 Prepared

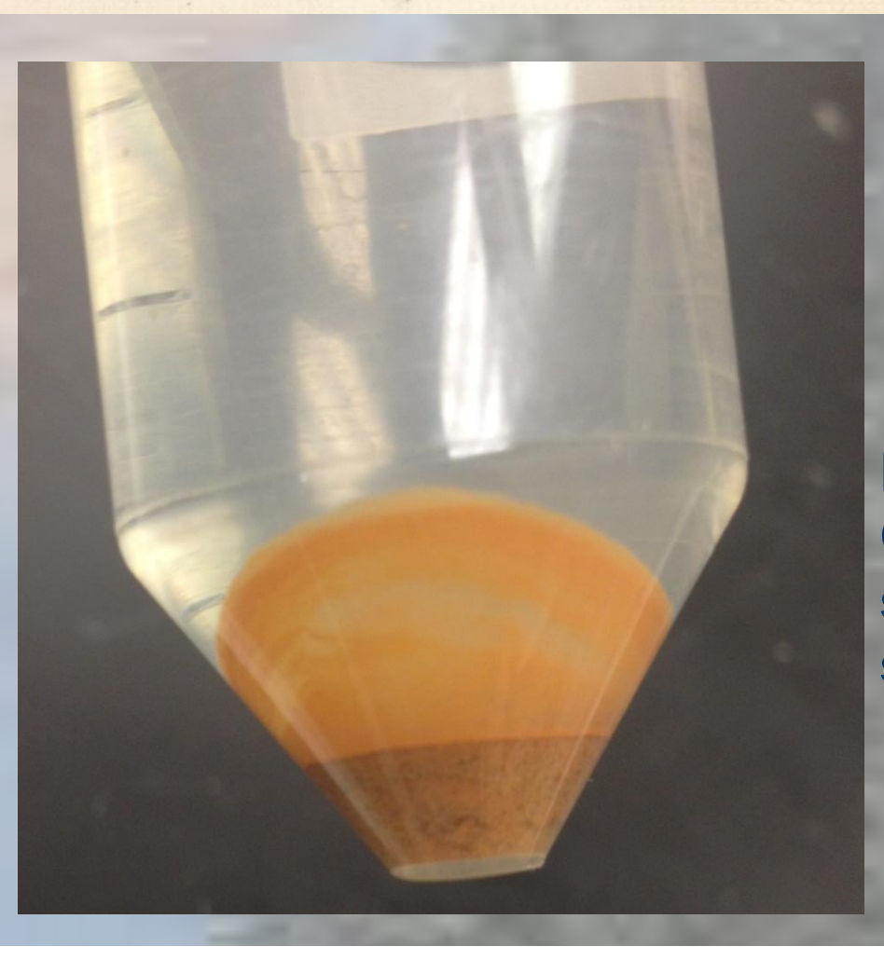
Figure R-2: Centrifuged sediment sample

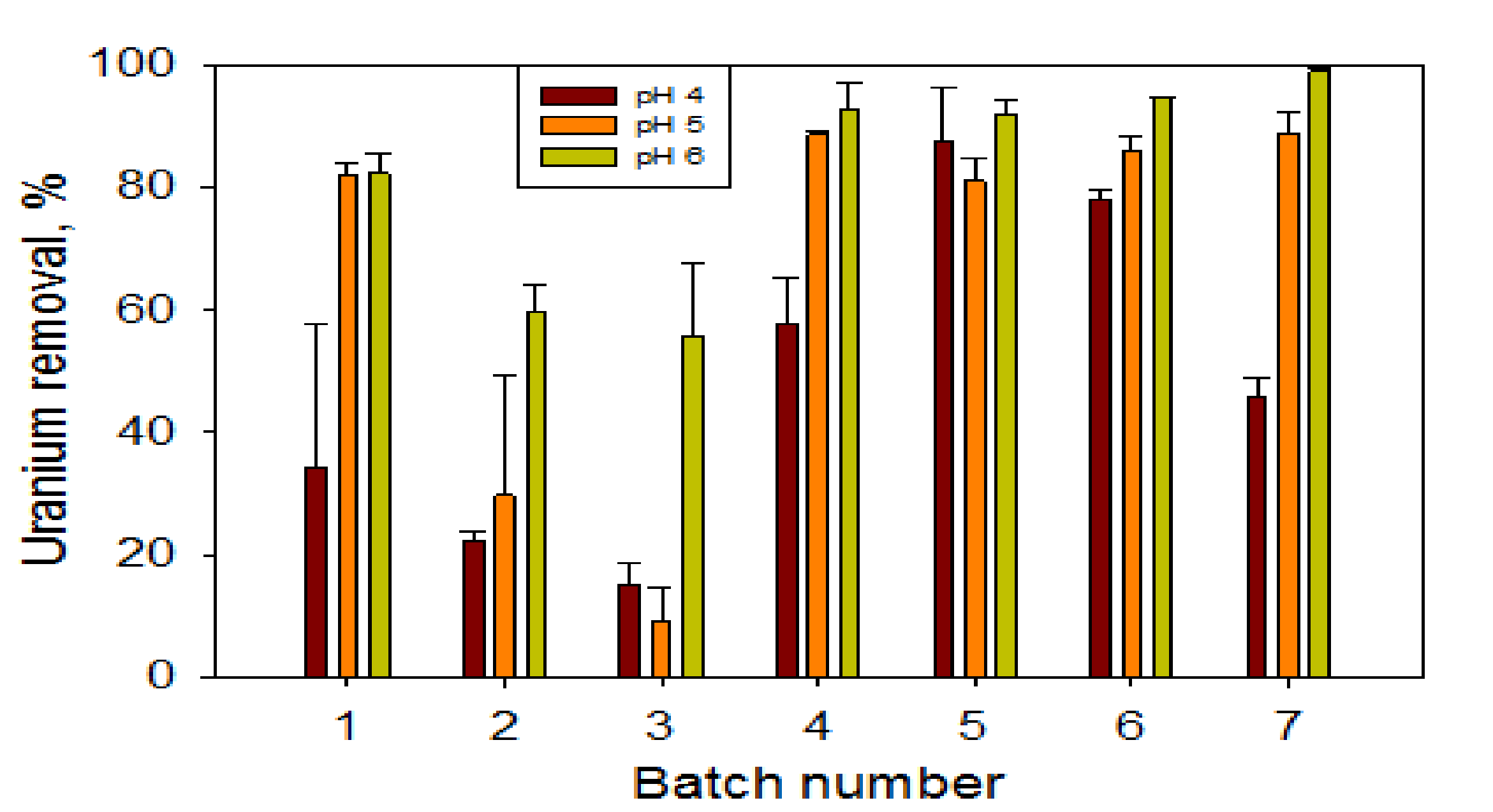

Figure R-3: Batches 4-6 Efficiency

Methods

EXPERIMENTAL MATRIX

The following binary, tertiary and quaternary systems will be evaluated at each pH value between pH 4-6 in the presence and absence of Humic Acid (HA) for the removal of U(VI) from the aqueous solutions:

PH 4-6 Adjusted Set	Constituents							
	SiO_2 3.5mM	Humic Acid (HA) 10 ppm	Sediments 1:20	Uranium U(VI) 0.5 ppm	Acid 0.1M HCL	Base 0.1M NaOH	Water H_2O	Total Volume
	ml	ml	mg	ml	ml	ml	ml	ml
Batch No. 1	2.24			0.01	Var.	Var.	17.75	20
Batch No. 2	2.24	2.00		0.01	Var.	Var.	15.75	20
Batch No. 3		2.00		0.01	Var.	Var.	17.99	20
Batch No. 4	2.24		400.00	0.01	Var.	Var.	17.75	20
Batch No. 5	2.24	2.00	400.00	0.01	Var.	Var.	15.75	20
Batch No. 6		2.00	400.00	0.01	Var.	Var.	17.99	20
Batch No. 7			400.00	0.01	Var.	Var.	19.99	20

Figure M-1: Acquired Soil

Figure M-2: Grain Sizes

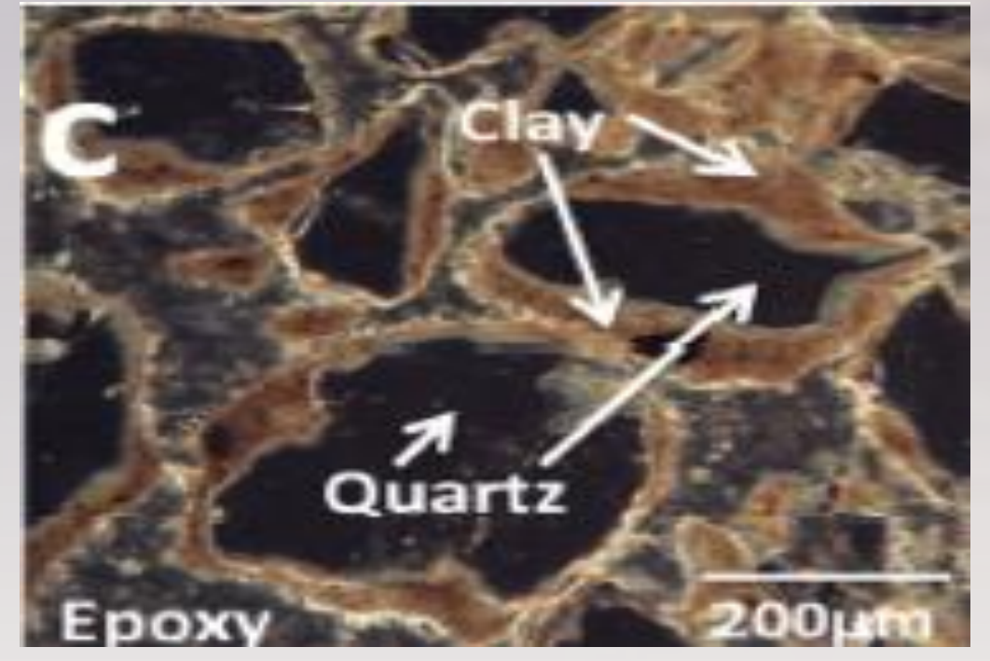

GENERAL PROCEDURES:

- Prepared colloidal silica stock solution at 2000 ppm in non-reactive bottles (polypropylene) to be injected in batch 1, 2, 4, and 5.
- For batches 2, 3, 5, and 6, added Humic acid (HA) stock at 10 ppm.
- Prepared soil mixture by combining soil samples gathered from various depths ranging from 60-105 ft.
- Prepared a 60 gram soil mixture using 10 grams of each of the 6 soil depths.
- Samples 4, 5, 6 and 7 each contain 400 mg of a soil/solution ratio of 1:20.
- Amended test solutions with 0.5 ppm U(VI), using a 1000ppm standard.
- Adjusted pH using 0.1M HCl or 0.1M NaOH.
- Each sample was prepared in triplicate.
- Centrifuged and analyzed via KPA and ICP.

Discussion

- At lower pH values silica (Si) and humic acid (HA) create good synergy in the presence of sediment.
- The synergy of Si and HA seems inversely related to the increase of pH value.
- In combination with sediments Si showed lower results on U removal than HA at lower pH levels.
- Attenuation of U(VI) via sediment sorption increases with pH.
- Sediment bearing samples with Si showed higher U removal at lower pH.
- HA slightly reduced U adsorption at higher pH values.
- The primary benefit of this study is to determine the most efficient means of reducing U(VI) using In situ adsorption.
- This research will aid in returning the ground water system to a natural pH while attenuating U(VI).

Future Work

- Analyze sediments' surface composition via scanning electron microscopy and energy-dispersive-spectrometry (SEM-EDS).
- Test to determine the effect of silicate solutions on the immobilization of U(VI).
- Perform experiments increasing the concentration of HA in the presence of sediment to analyse for efficiency of U(VI) adsorption.

Acknowledgements

- DOE/FIU Science & Technology Workforce Development Initiative for providing research opportunities.
- DOE-EM for support of this research.
- Drs. Miles Denham and Brian Looney for their support.
- Dr. Leonel Lagos for this research opportunity.

FIU Applied Research Center
FLORIDA INTERNATIONAL UNIVERSITY

A Study of Cell Viability on DOE Hanford Soil Isolates: Effect of U (VI) and Bicarbonate

Paola Sepulveda, BS, Biomedical Engineering
(Graduate Student, DOE Fellow)

Background

- In 2005, a study began to identify and evaluate remedial strategies to sequester uranium contamination in the subsurface.
- The injection of a polyphosphate amendment in hot spot areas significantly reduces the inventory of available uranium that contributes to the groundwater plumes.
- This *in situ* remediation process via polyphosphate injections into contaminated groundwater results in the formation of uranyl phosphate solid phases in the soil and groundwater, such as autunite.
- Because autunite sequesters uranium in the oxidized form, U(VI), rather than forcing reduction to U(IV), the possibility of subsequent re-mobilization of uranium is prevented.
- In addition, formed autunite, as a phosphorus-containing mineral, can attract bacteria to liberate phosphorus, meeting their nutrient requirements and causing U release back into the environment.
- The significance of bacteria-uranium interactions has been illustrated by focusing on three bacterial strains of *Arthrobacter* sp, isolated from Hanford Site soil.
- This research was extended to investigate the stability of the autunite mineral in oxidized conditions pertaining to the Hanford Site, and to study the effect of the *Arthrobacter* oxydans SMCC G968 strain on the U (VI) release from autunite.

Objectives

- Inspect bacterial surfaces after exposure to U (VI) in the bicarbonate-bearing synthetic groundwater solution via atomic-force microscopy (AFM)
- Investigate cell viability via Live/Dead Fluorescent assay

Methodology

- Bacterial cell growth
  - 5% PTYG liquid culture media
  - Two days
- Log 7 cells/mL of the bacterial stock solution was incorporated with uranyl nitrate and SGW media to create individual samples for analysis.
- Samples for viability assessment were similar to samples used for AFM imaging.
  - 3 µL of the dye mixture was added for each mL of the bacterial suspension.
  - Equal parts of SYTO9 and propidium iodide
- The samples were incubated at room temperature in the dark for 15 minutes and washed 3 times to prevent a bright background when imaging.
  - Five microliters of the stained bacterial suspension was placed on a microscope slide and allowed to dry for 1 hr before being imaged via a fluorescence microscope.

Results

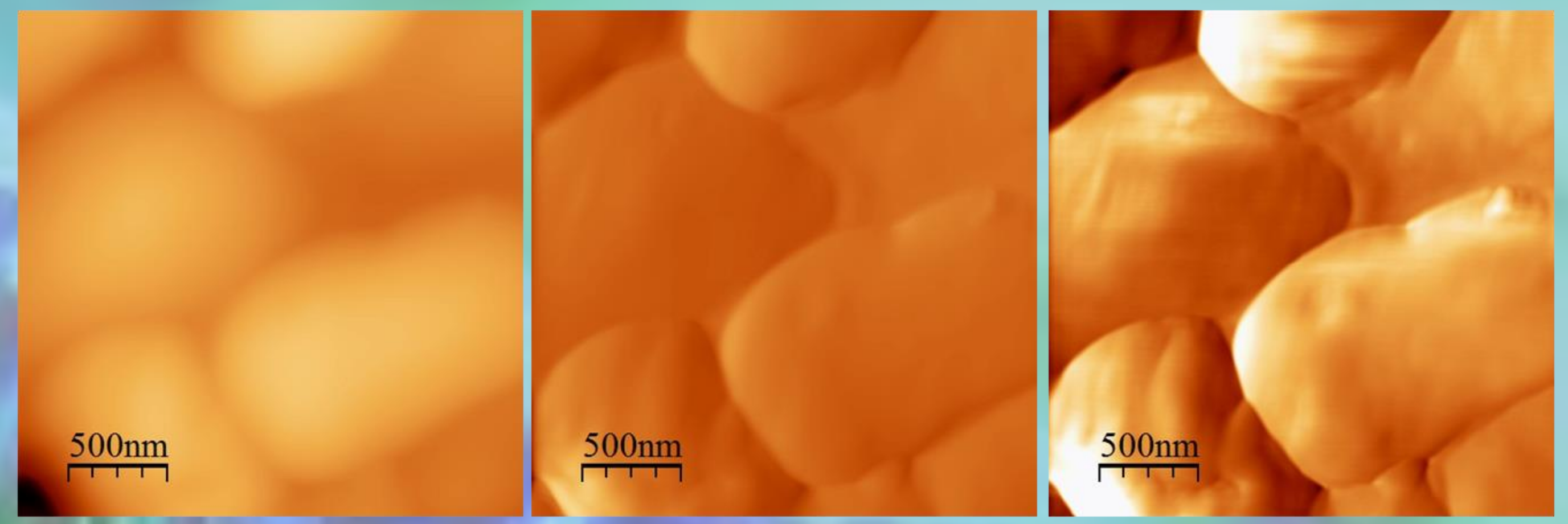

Figure 1. G968 control sample (scan size 2.5 x 2.5 µm^2) illustrating smooth bacterial surface. The topographic image on the left, deflection image in the middle and friction image on the right.

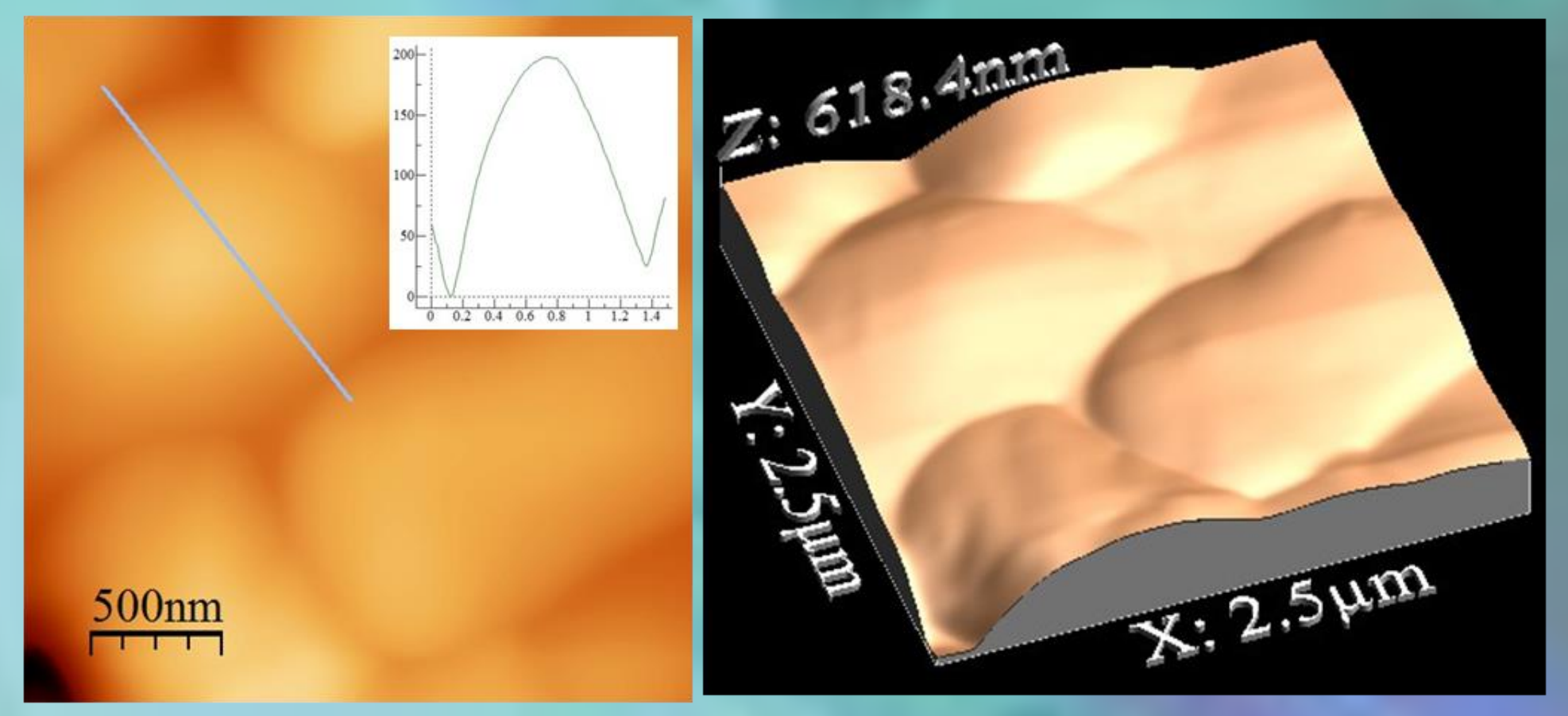

Figure 2. G968 control sample with a maximum height of 198. The profile plot is on the left with the 3D topographic image on the right.

- Adhesion forces are sensitive to modifications in the surface; so, a force spectroscopy analysis was performed to gain a better understanding of the interactions at the atomic level.
- There is an inverse relationship between the adhesion forces and the concentration of uranium; as the concentration of uranium increases, the adhesion forces will decrease exponentially.
- When bicarbonate is present within the solution, the adhesion forces showed similar values to that of the control sample when no uranium is present.

	Adhesion (nN)	SD
Control	11.6*	1.68
5ppm U, 0 mM HCO3	7.14*	0.26
5ppm U, 5 mM HCO3	9.51	1.2
10ppm U, 0 mM HCO3	5.54	4.3
10ppm U, 5 mM HCO3	4.88	2.3

Table 1. Adhesion Forces for Arthrobacter sp. G968
*Data was obtained from the 2010 Year End Report and recent publications (Katsenovich et al. 2012a, Katsenovich et al. 2012b)

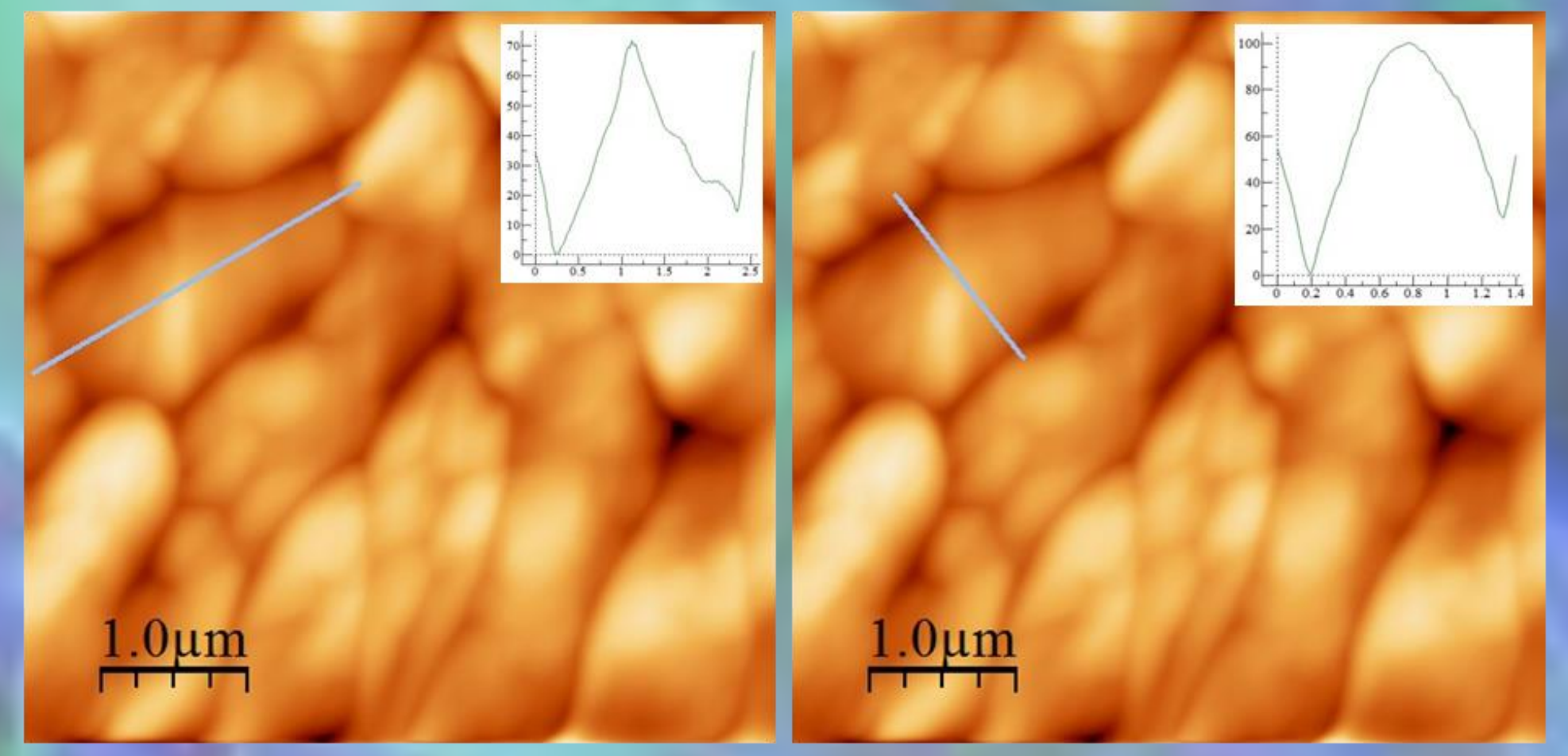

Figure 3. 10 ppm U (VI) and 0 mM bicarbonate. The profile heights: 70-90 nm.

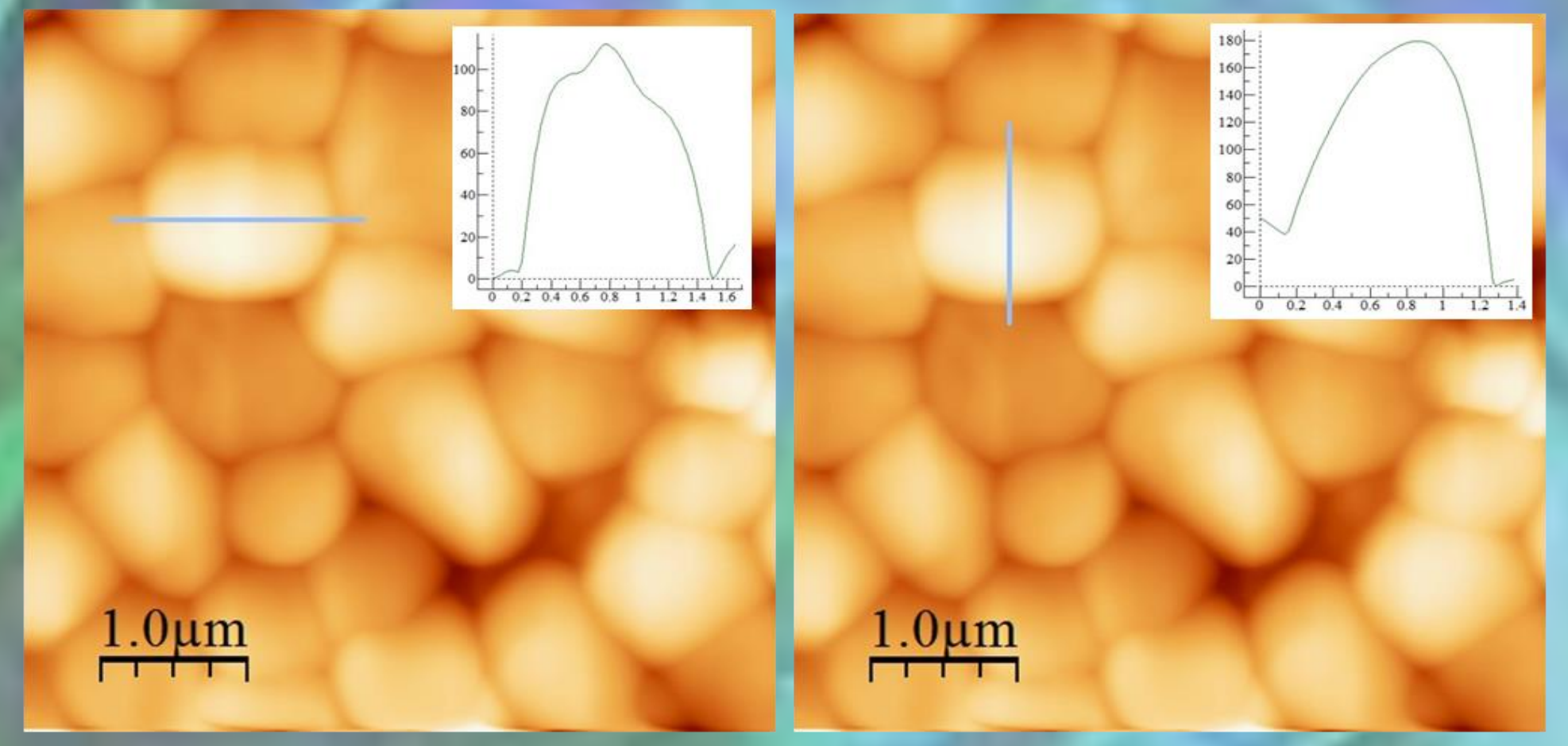

Figure 4. 10 ppm of U (VI) and 5 mM of bicarbonate. The profile heights: 110-180 nm.

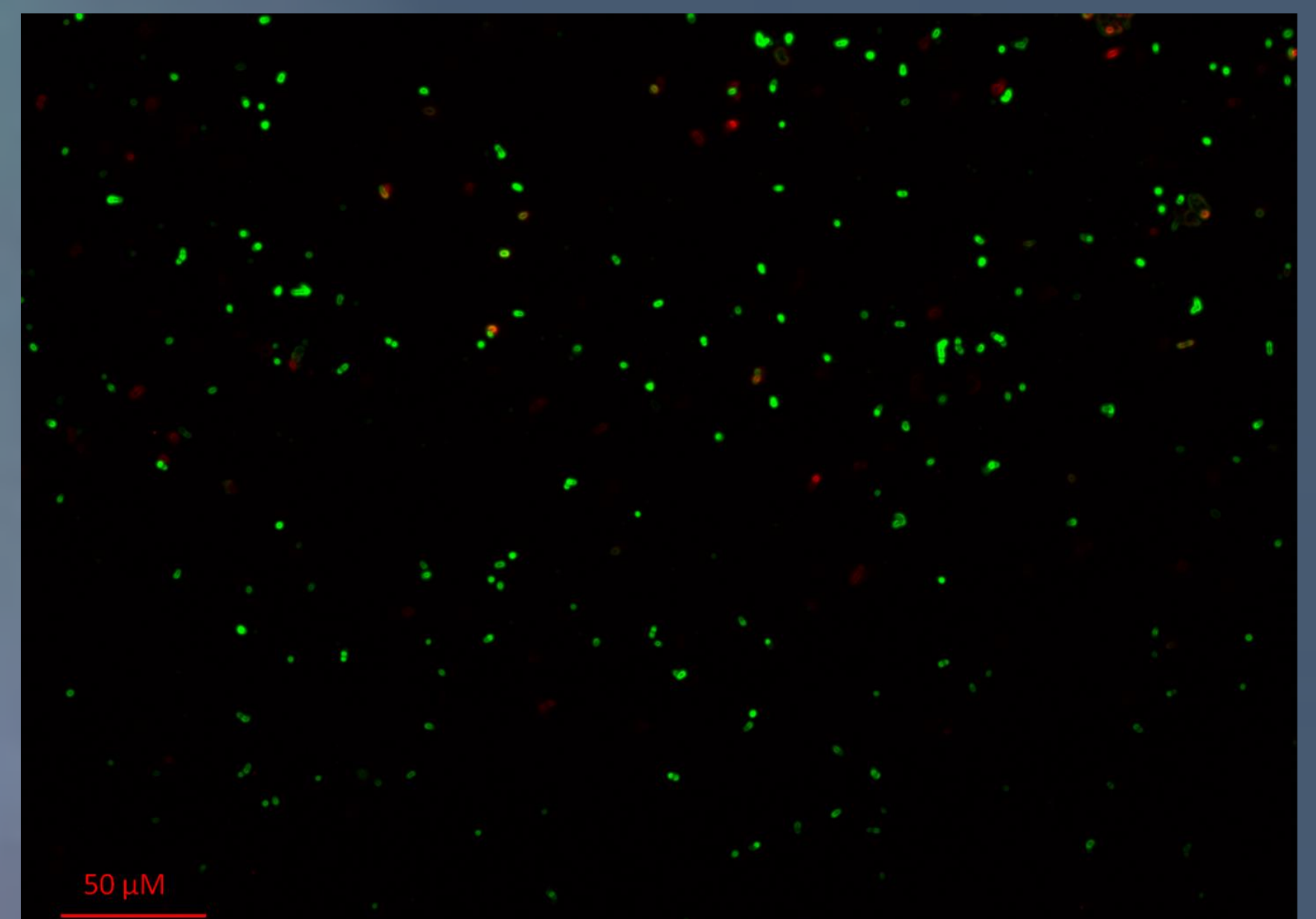

Figure 5. Live/Dead assay sample containing 10 ppm of U (VI) with no bicarbonate. This sample illustrates a higher concentration of dead cells compared to the figure below.

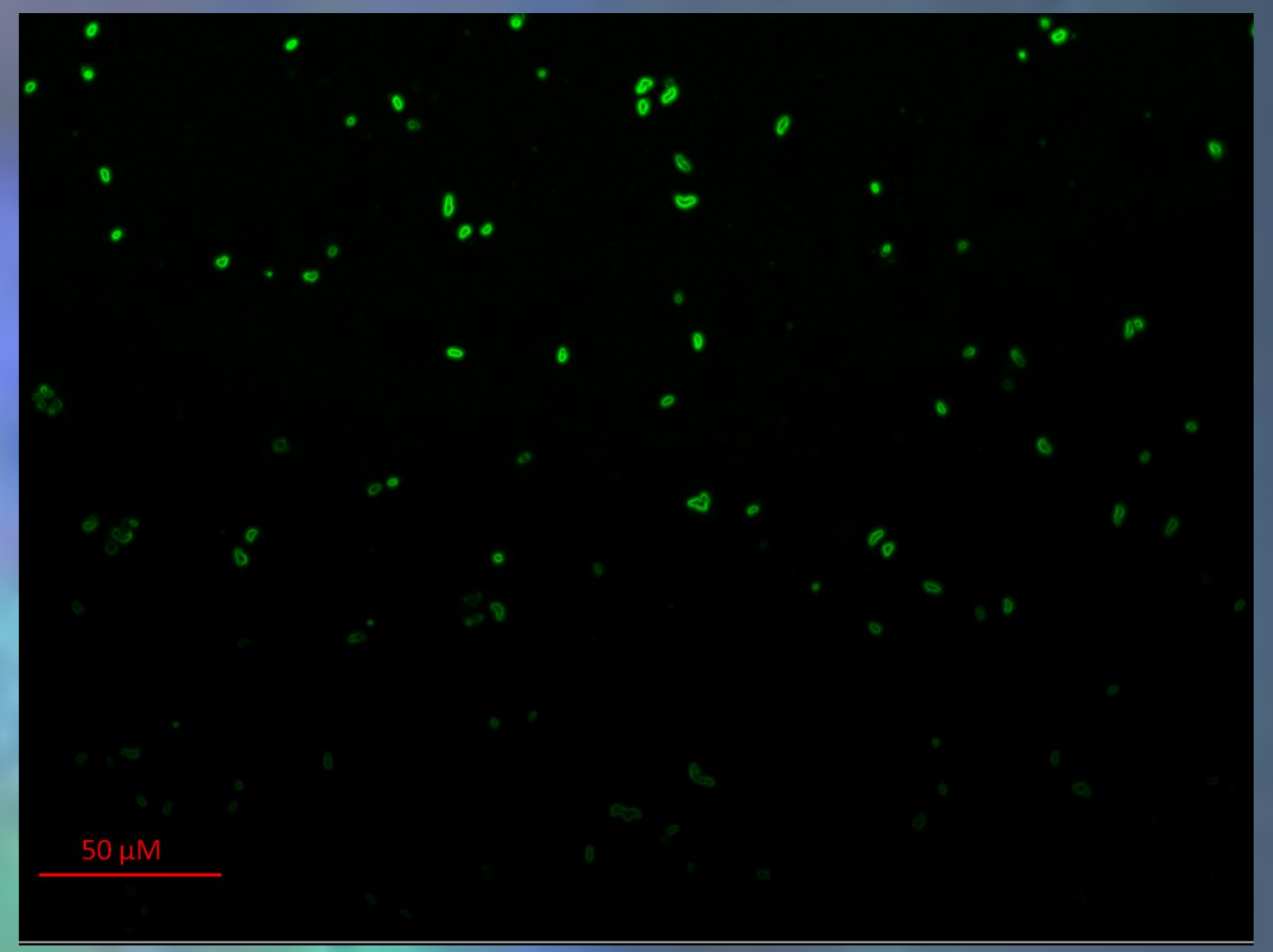

Figure 6. Live/Dead assay of sample containing 10 ppm of U (VI) with 5 mM bicarbonate. This sample illustrates a large concentration of live cells.

- When calculating the viability of cells for each sample, it has been found that there is not much difference between the varying concentration of uranium and bicarbonate.
- Each sample exhibited a ratio of live cells greater than 95% and when making a comparison between the sample containing 10 ppm of U (VI) with and without bicarbonate, it is apparent that the sample containing bicarbonate contains a higher ratio of live cells.

Discussion

- Live/Dead analysis shows that despite the concentration of uranium and bicarbonate present in the solution, each sample exhibited a ratio of live cells greater than 95%.
- Performing a cell viability assessment via culture plates, results demonstrated that although the bacterial cells established intact cytoplasmic membranes, resulting in viable cells for live/dead analysis, the cells that are exposed to uranium with no bicarbonate experienced a viable but nonculturable state, that is, experienced low levels of colonies when plated.
- Force spectroscopy results demonstrate that as uranium is added to the media, the adhesion force parameter decreases.
- Furthermore, the height provided from profile plots reveal that samples containing bicarbonate have a higher profile height, resulting in a much smoother surface. Thus, samples exposed to uranium with no bicarbonate are mostly viable, but are not alive. In contrast, samples containing bicarbonate have a reduced height and small cellular size but are alive and have acclimated to withstand uranium toxicity.

Acknowledgements

Dr. Yelena Katsenovich (ARC-FIU)
Dr. Leonel Lagos (ARC-FIU)
Funds provided by DOE DE-EM0000598 grant
DOE-FIU Science and Technology Workforce Development Program

FIU
Applied Research Center

Characterization of the Uranium-Bearing Products of Novel Remediation Technologies

Robert Lapierre (Graduate Student –Chemistry, DOE Fellow), Dr. Yelena Katsenovich
Applied Research Center, Florida International University

Background

- Hanford, WA has seen copious amounts of contamination from leakage and spillage of radiological waste
- Uranium is a primary vadose zone contaminant in the Hanford 200 Area and is a potential future source of groundwater contamination to the Columbia River
- Remediation efforts include employing novel technologies to sequester the flow of radiological contaminants such as *in situ* subsurface pH manipulation using NH_3 gas
    - Injection of ammonia gas causes an increase pore water pH inducing the dissolution of soil minerals into the aqueous system. The subsequent return to natural pH conditions is believed to result in the recrystallization of soil minerals and the co-precipitation of uranium

Objectives

- Characterization of uranium bearing precipitates produced by the NH_3 injection method
    - Deduce how uranium is incorporated into the product
    - Discern the chemical formula for the uranium-based phases

Methodology

- Samples prepared from a solution prepared to mimic conditions observed at the Hanford 200 Area
    - Varying calcium and bicarbonate concentrations
    - Previous studies looked at the effect of time in solution
- Dried samples analyzed by SEM-EDS
    - BEC mode and EDS for uranium identification
- Micro-Raman Spectroscopy performed to attempt to identify the phases of the sample by comparison to reported spectra
- The samples were pulverized and mounted to a custom designed plastic sample holder for XRD analysis
    - Method blanks were prepared for both samples (*sans uranium*)
    - Comparisons were done using *Match!* and references from ICDD powder diffraction files

Results

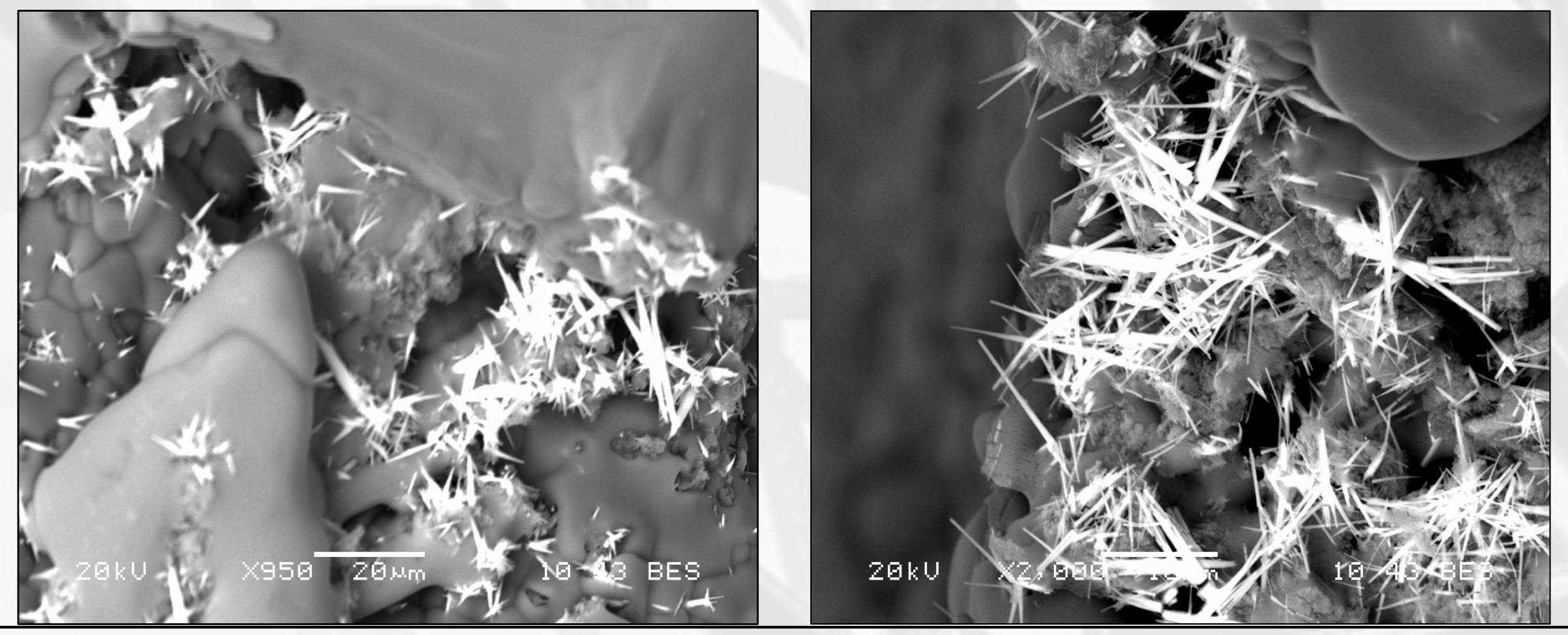

Backscatter SEM images of samples prepared with (L) and without (R) calcium showing the U-rich crystal-like forms

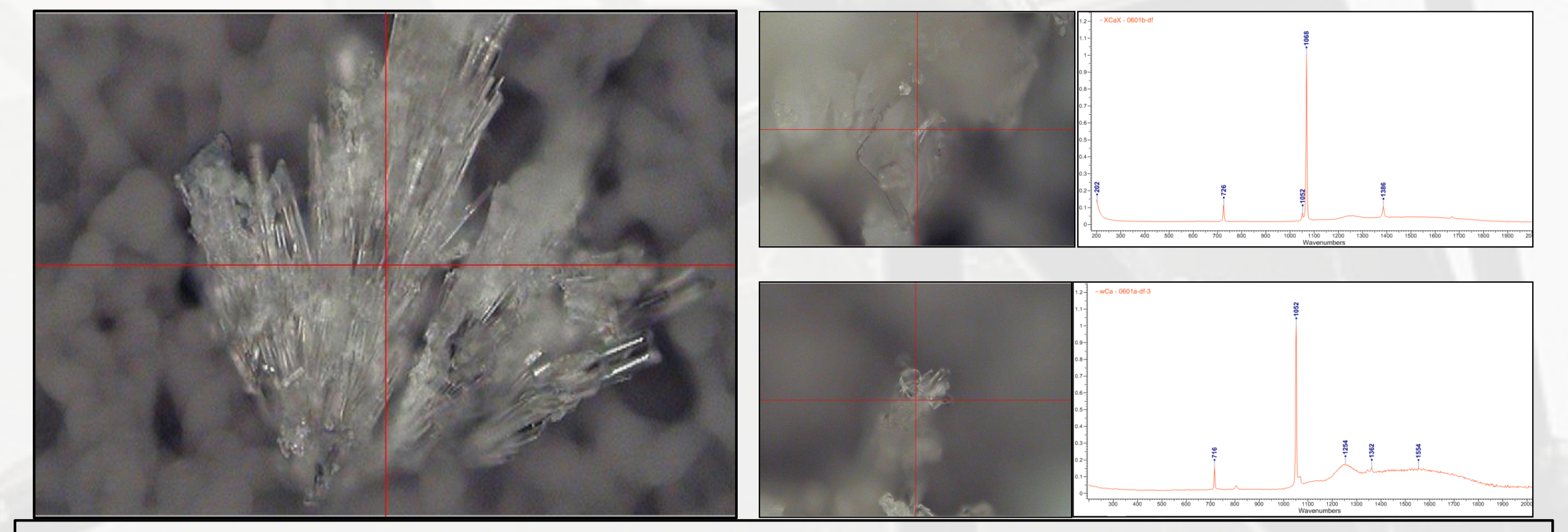

Micro-Raman image and spectra for samples prepared with (top) and without (bottom) calcium

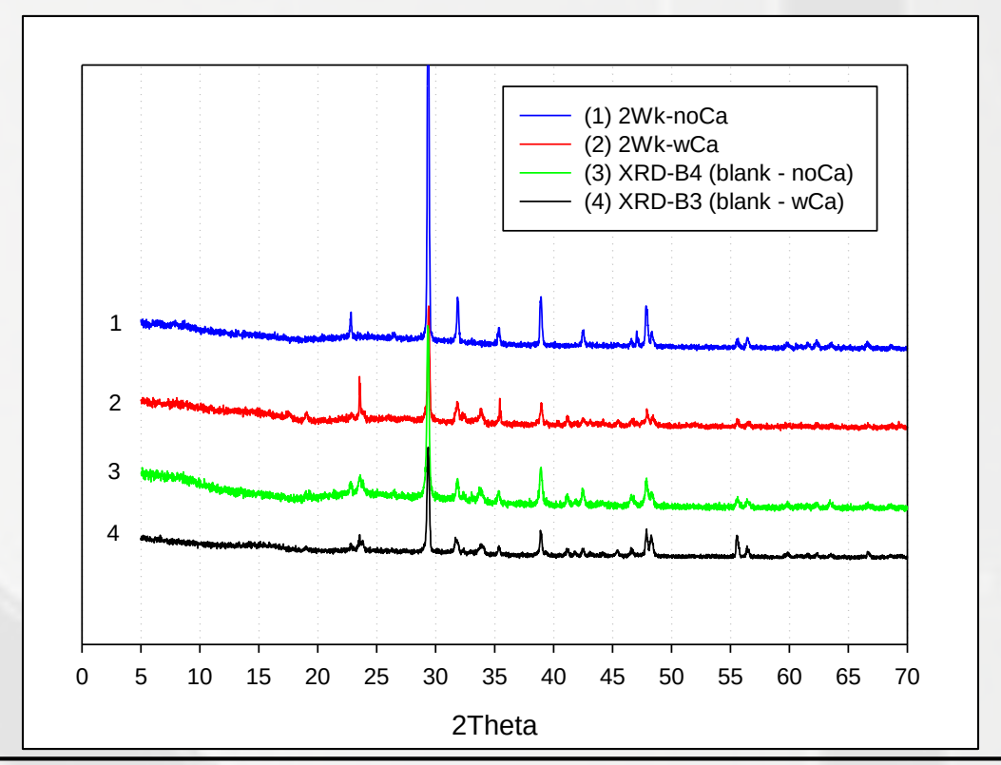

Comparison of XRD patterns for samples prepared with and without calcium & corresponding U-free blanks

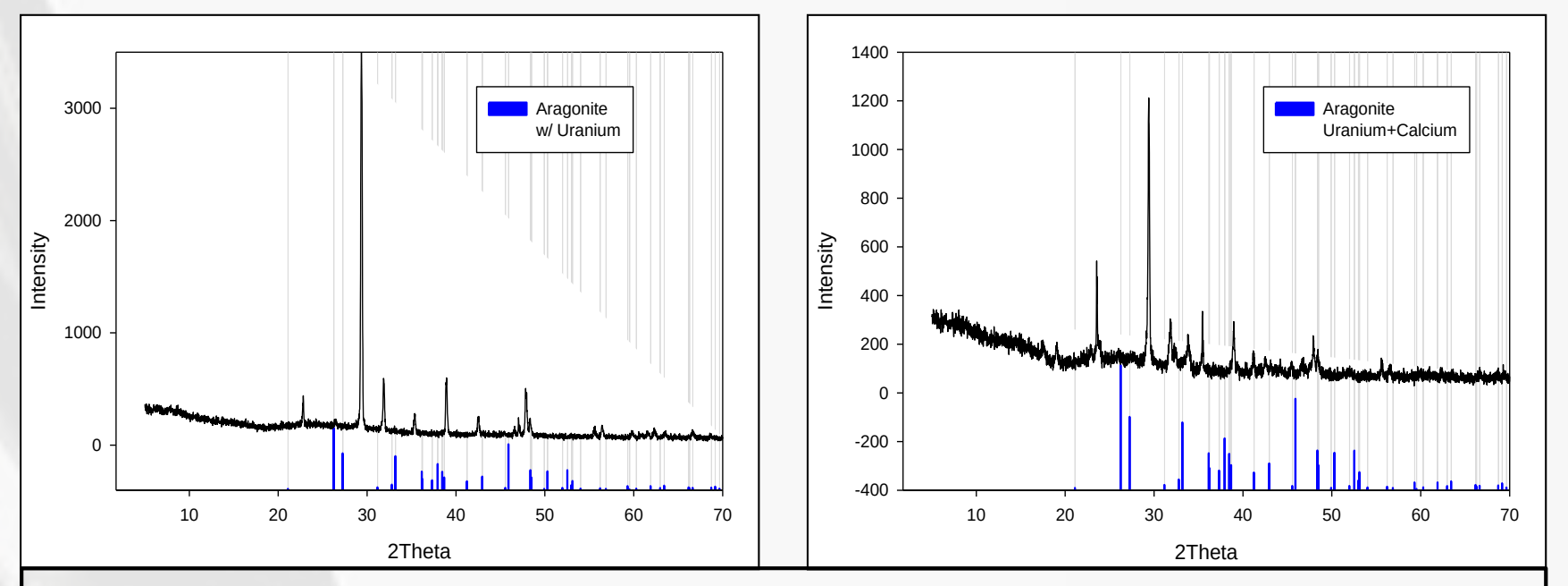

Comparison of XRD patterns for uranium-containing sample ($^{w}/$ & $^{w}/_{o}$ Ca) to the pattern for aragonite ($CaCO_3$)

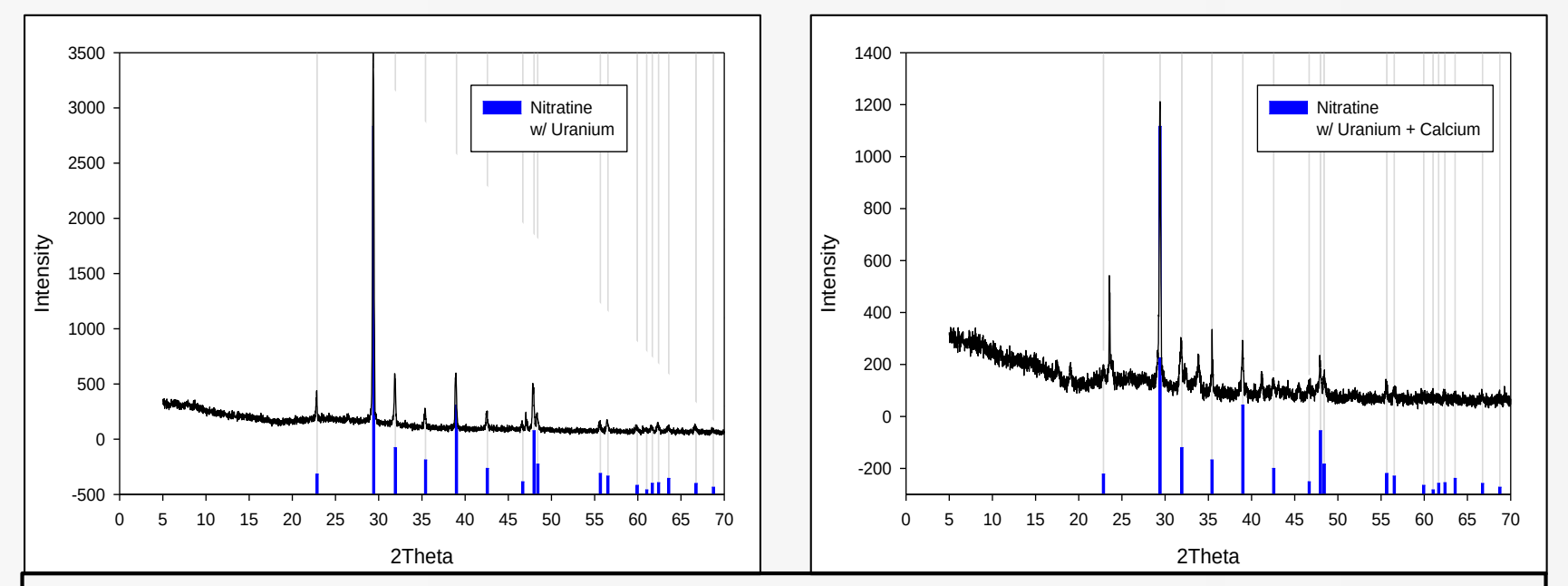

Comparison of XRD patterns for uranium-containing sample ($^{w}/$ & $^{w}/_{o}$ Ca) to the pattern for nitratine (*$NaNO_3$*)

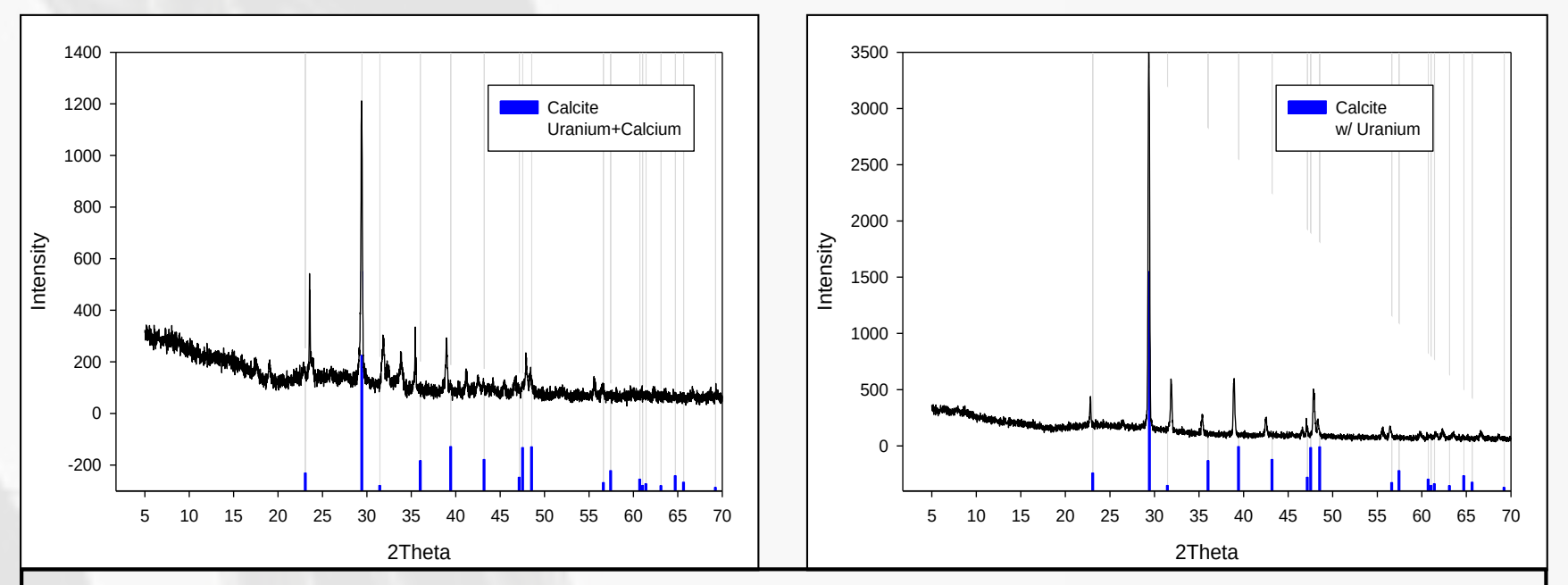

Comparison of XRD patterns for uranium-containing sample ($^{w}/$ & $^{w}/_{o}$ Ca) to the pattern for calcite ($CaCO_3$)

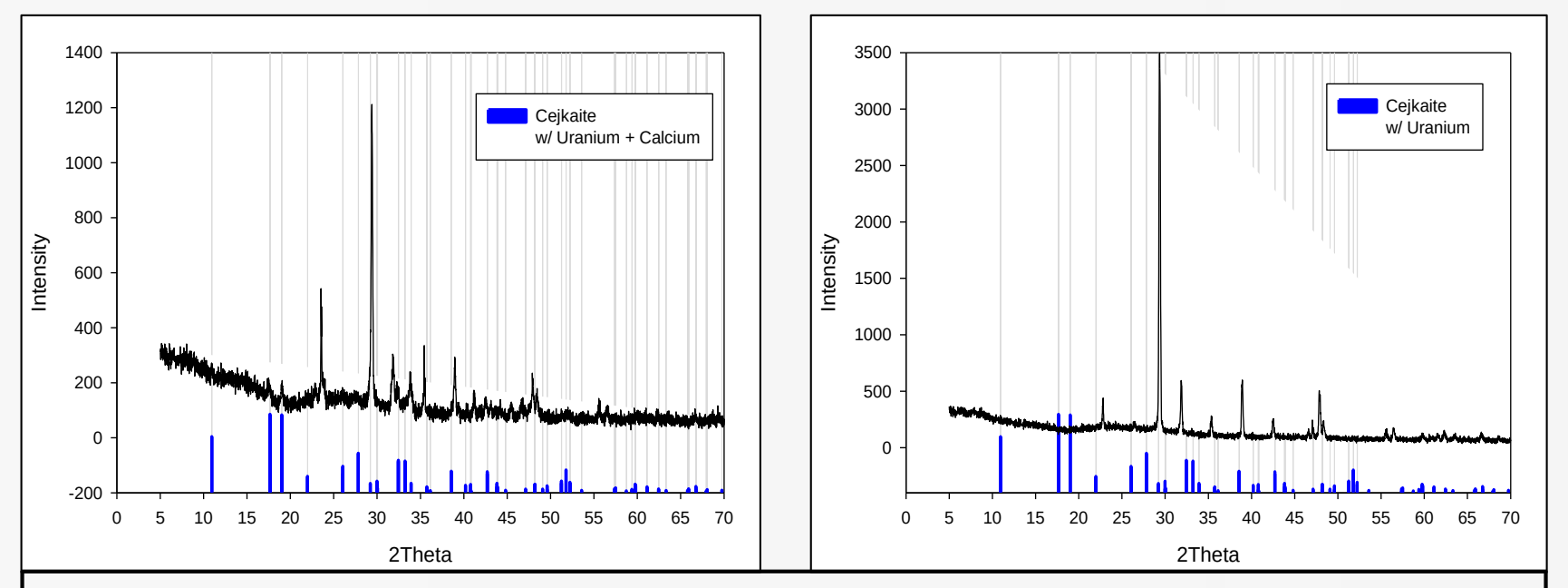

Comparison of XRD patterns of uranium-containing sample ($^{w}/$ & $^{w}/_{o}$ Ca) to the pattern for cejkaite (*$Na_4(UO_2)(CO_3)_3$*)

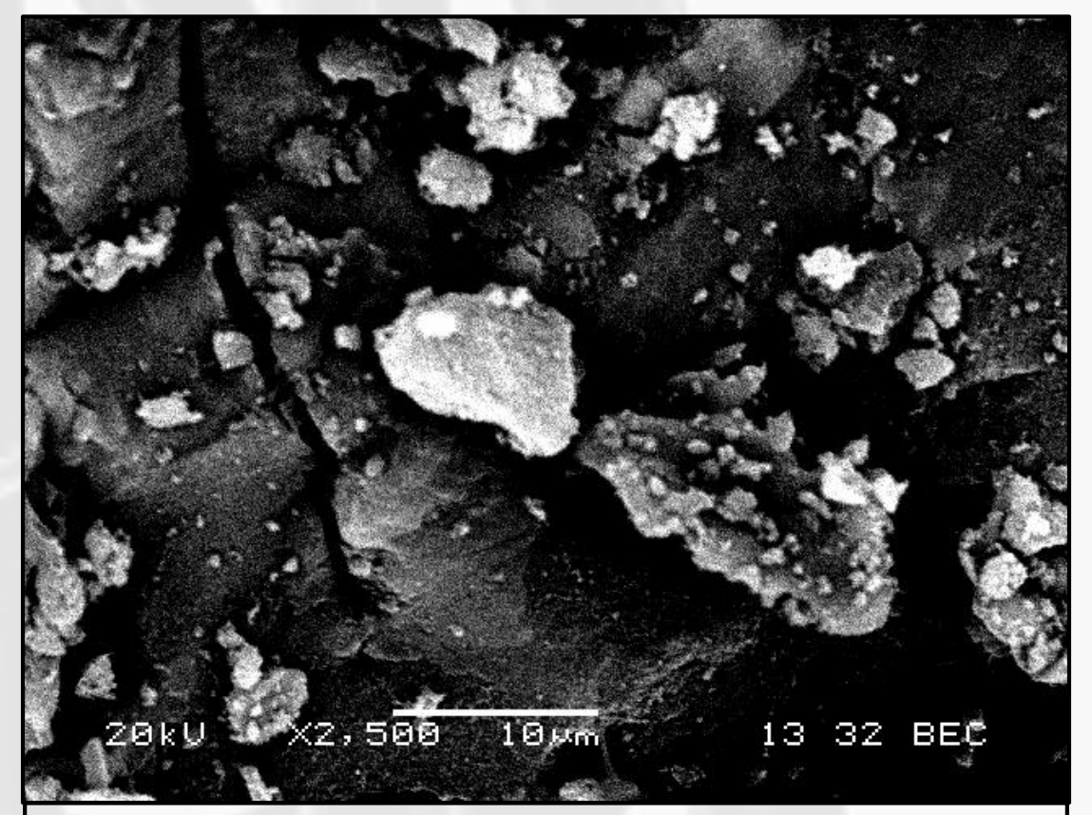

SEM image of the pulverized $^{w}/$ Ca sample after XRD analysis (*no uranium identified*)

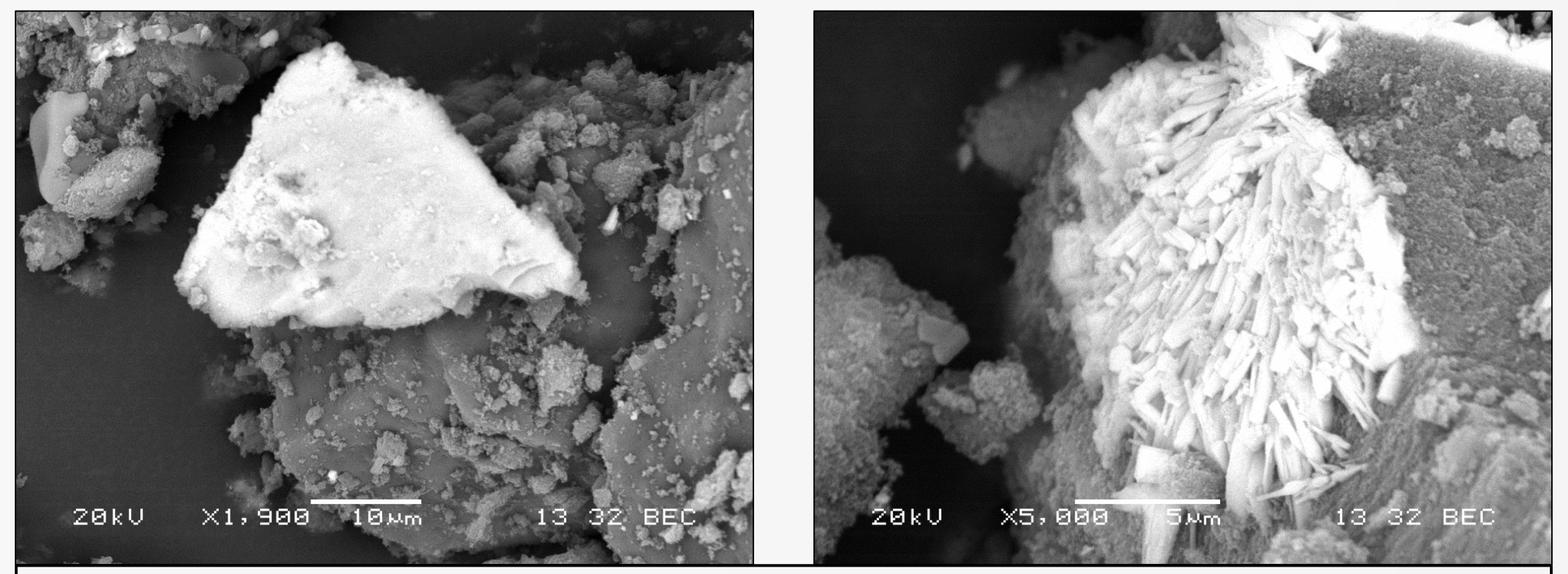

SEM image of the uranium-rich areas of the pulverized $^{w}/$ Ca sample after XRD analysis *(identified via EDS)*

Discussion/Conclusions

- SEM, in backscatter electron capture mode, of dried samples allowed areas of higher average atomic number to be identified. EDS analysis supported the prediction that these areas would have an elevated concentration of uranium.
- Micro-Raman Spectroscopy of the samples revealed bands, at 800 cm^{-1} & 1000 cm^{-1}, which are consistent with reported values/ranges for the stretches of $(UO_2)^{2+}$ and $(CO_3)_2^{-}$, respectively.
- Powder XRD analysis confirmed the presence of crystalline material in the precipitate.
    - *Match!* software and PDF comparisons suggest that nitratine ($NaNO_3$), the most prominent peak of which occurs at $2\Theta = 29$, overwhelmingly dominated all samples.
    - Speciation predictions in similar studies suggested that calcium carbonate forms (i.e.: calcite, vaterite, & aragonite) would be produced but comparisons of their most prominent peaks showed little to no match.
    - Though it was not included in predictions, cejkaite ($Na_4(UO_2)(CO_3)_3$) has emerged as a potential identity of the uranium-bearing phase that was visualized by SEM/EDS.
        - Significant matches for the 2 most prominent peaks ($2\Theta \approx 17.5$ & 19) and a potential match for the 3rd ($2\Theta \approx 11$) obscured in elevated noise early in the pattern.
- SEM-EDS analysis (post-XRD) confirmed presence of uranium-rich phases in the sample with calcium. *None detected in the sample without calcium*.

Future

- The characterization of the major U-phases was hindered by the contribution of unexpected amounts of nitratine formed.
    - The sample preparation will be modified to minimize sodium content and increase uranium concentrations

Acknowledgements

- Dr. Leonel Lagos
- DOE-FIU Science and Technology Workforce Development Program
- Tom Beasley of FIU-FCAEM

Microcosm Study on Mineralogical Changes of post Molasses Injection with Savannah River Site (SRS) F-area Sediments

Valentina Padilla (DOE Fellow), Dr. Yelena Katsenovich

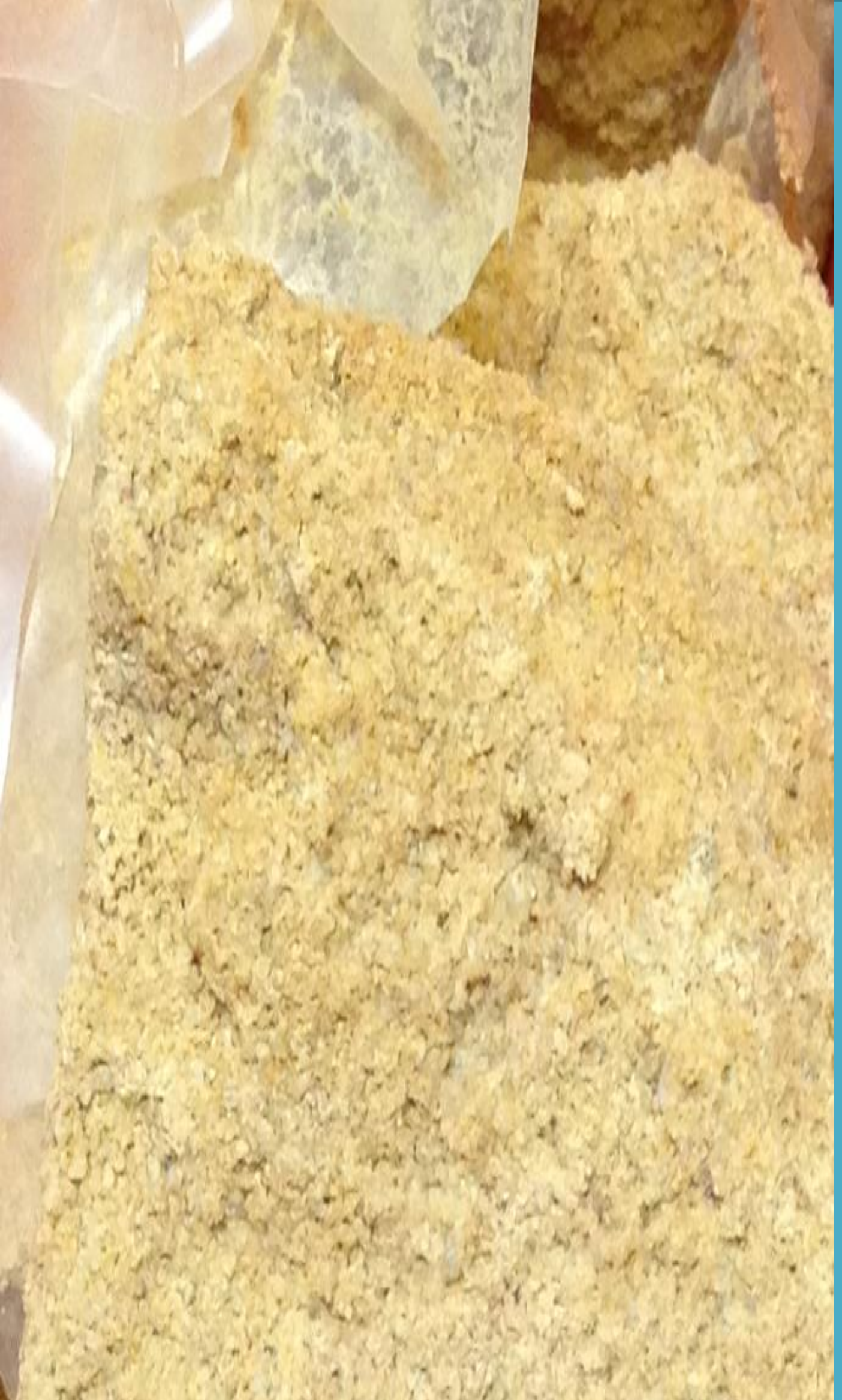

ARCADIS Technology

- Enhanced Anaerobic Reductive Precipitation (EARP)
  - Targets metals and radionuclide contaminants
- Known as In situ Reactive Zones (IRZs)
- Works by introducing a carbon substrate (molasses) to the groundwater advective flow distribution
- Periodic injections (April 2010 through January 2011)
- Produced anaerobic conditions through microbial action
- Uranium is a redox-sensitive radionuclide
  - Mobility gets minimized
  - Aqueous U(VI) ➡ Insoluble U(IV) form
- As of March 2011:
  - Evidence of methanogenesis
  - Rebound to less-reducing condition beginning to occur at the edge of the reactive zone
- Project was left unfunded
  - Period where re-oxidation occurred was left unmonitored
  - What effect did this have on reduced uranium?
    ➡ the longevity of the technology could not be proven

F-Area Depth Profile Analysis

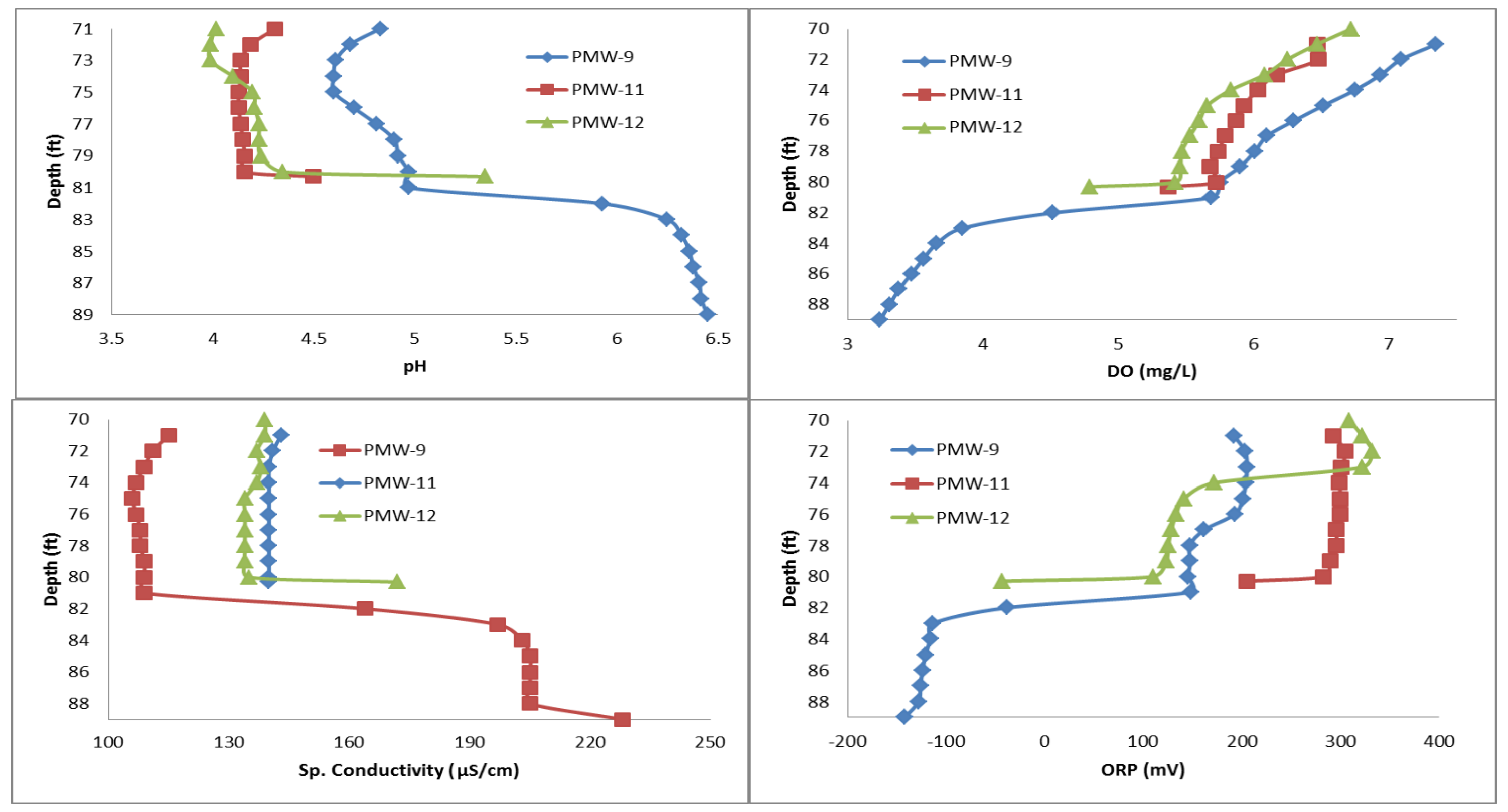

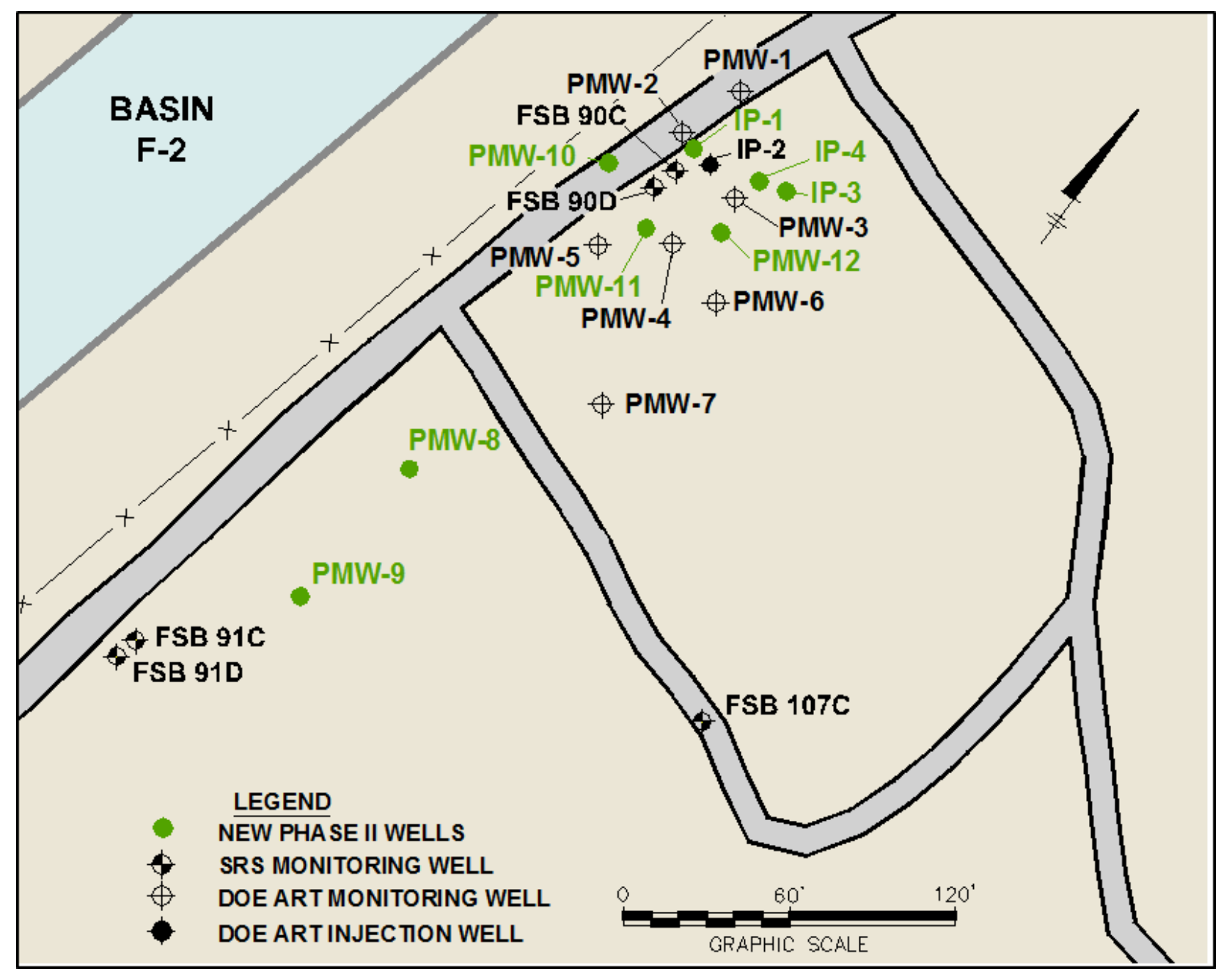

Objective

The main goal is to accomplish long term remediation to sequester contaminants in the subsurface without degrading the overall water quality or drastically changing the ecosystem of the region.

⬇

These experiments will also explain the types of reactions that might occur in the anaerobic aquifer.

Methodology

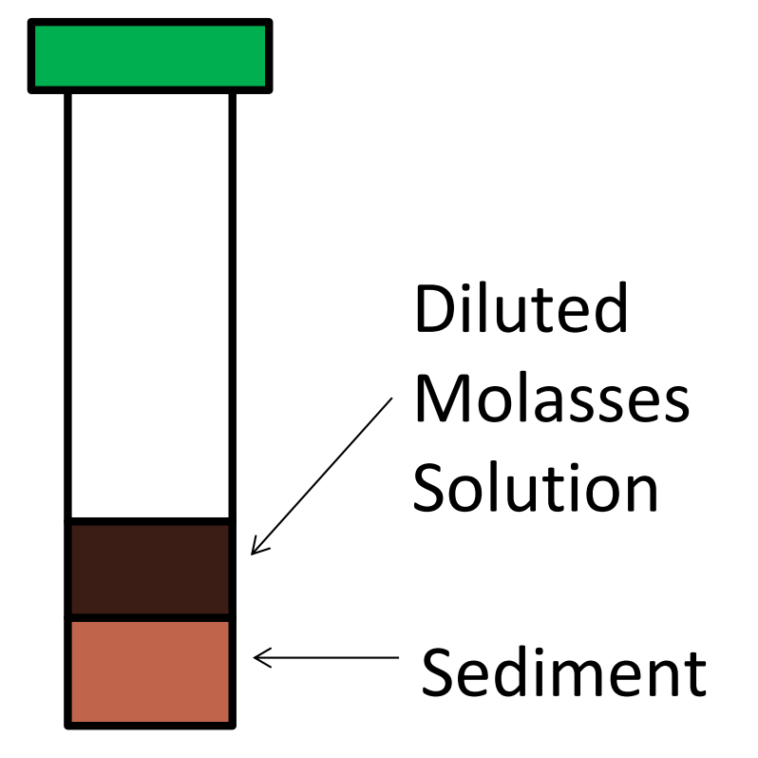

Samples contained:

- Enough sediment to occupy 10 mL
- 10 mL of diluted molasses solution (5%)
- Batch 2 was inoculated with bacteria from a local WWTP anaerobic digester

- Solid Phase → XRD
  - Samples are dried in their respective oxygenated environments
- Liquid Phase →ICP
  - Liquid is centrifuged
  - Supernatant is filtered (0.45 µm)

pH Changes

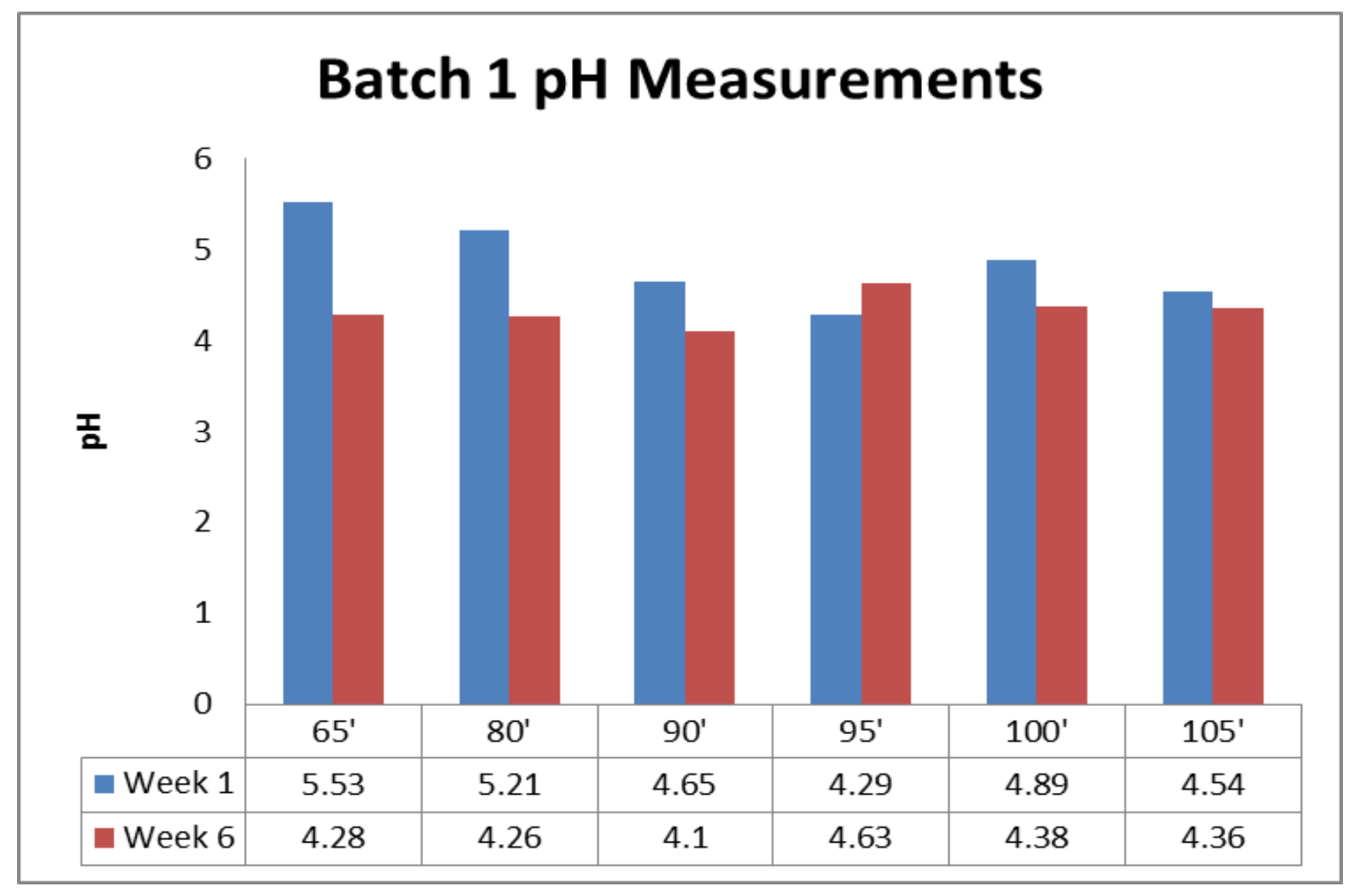

	65'	80'	90'	95'	100'	105'
🟦 Week 1	5.53	5.21	4.65	4.29	4.89	4.54
🟥 Week 6	4.28	4.26	4.1	4.63	4.38	4.36

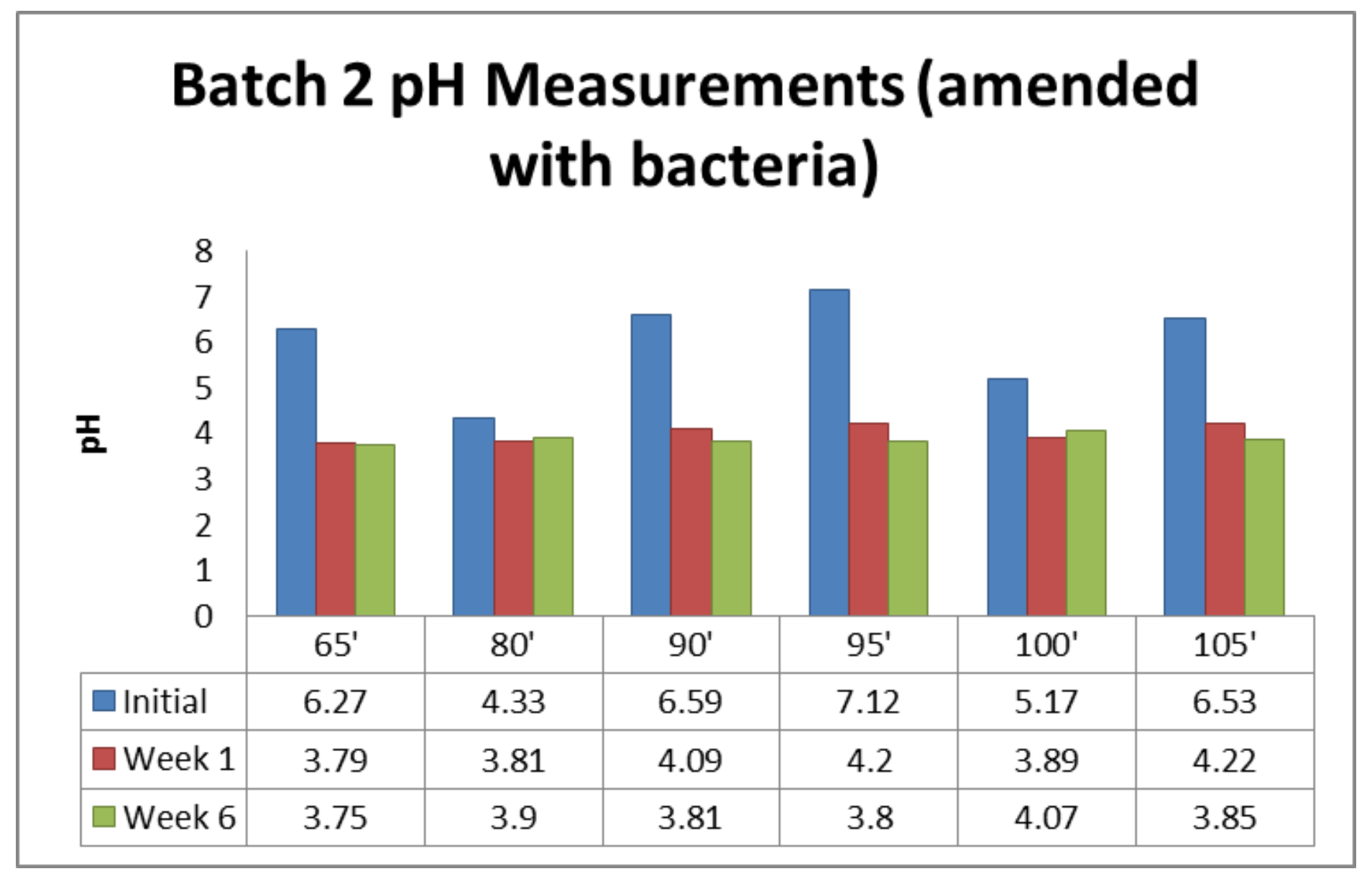

	65'	80'	90'	95'	100'	105'
🟦 Initial	6.27	4.33	6.59	7.12	5.17	6.53
🟥 Week 1	3.79	3.81	4.09	4.2	3.89	4.22
🟩 Week 6	3.75	3.9	3.81	3.8	4.07	3.85

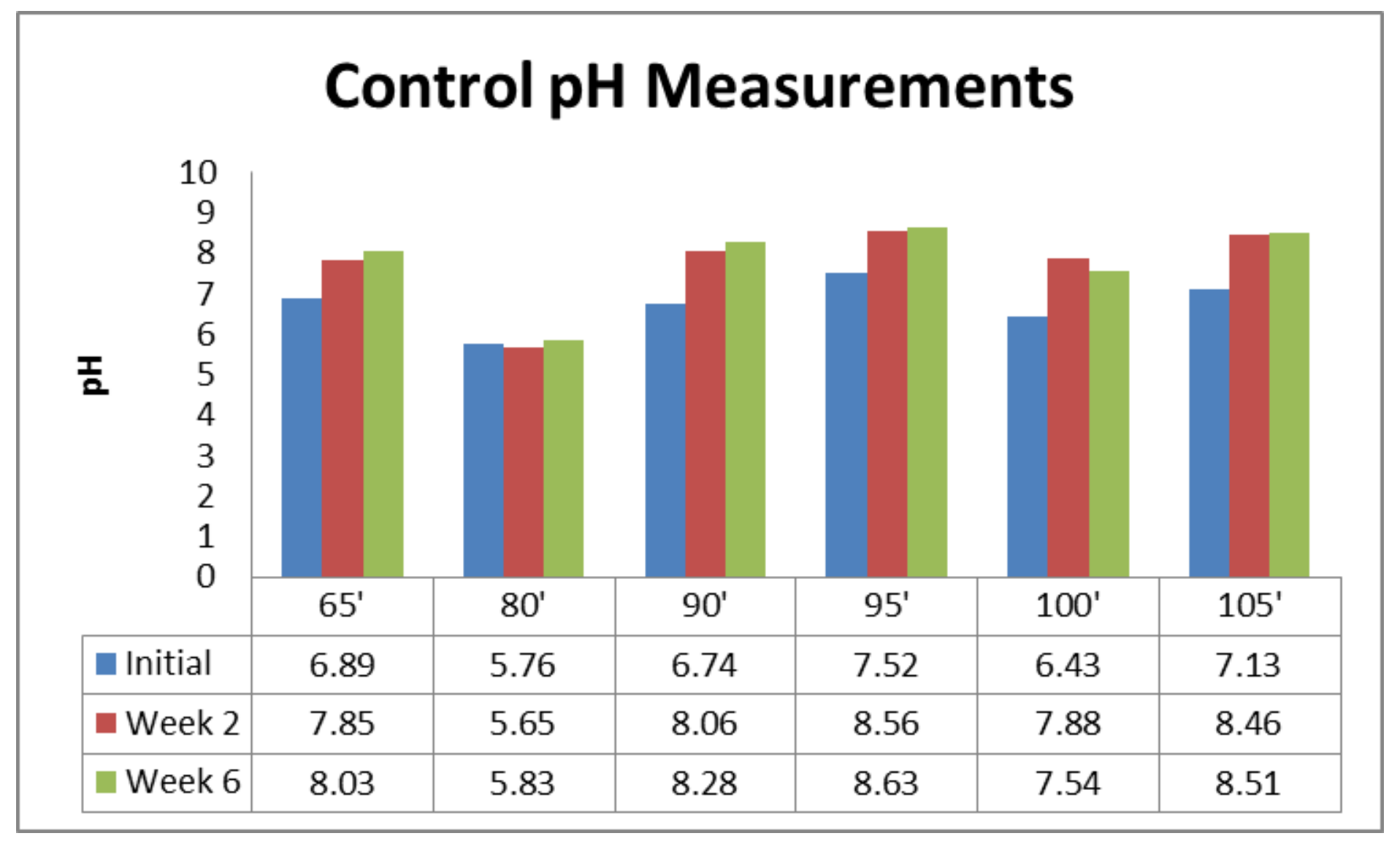

	65'	80'	90'	95'	100'	105'
🟦 Initial	6.89	5.76	6.74	7.52	6.43	7.13
🟥 Week 2	7.85	5.65	8.06	8.56	7.88	8.46
🟩 Week 6	8.03	5.83	8.28	8.63	7.54	8.51

XRD Analysis

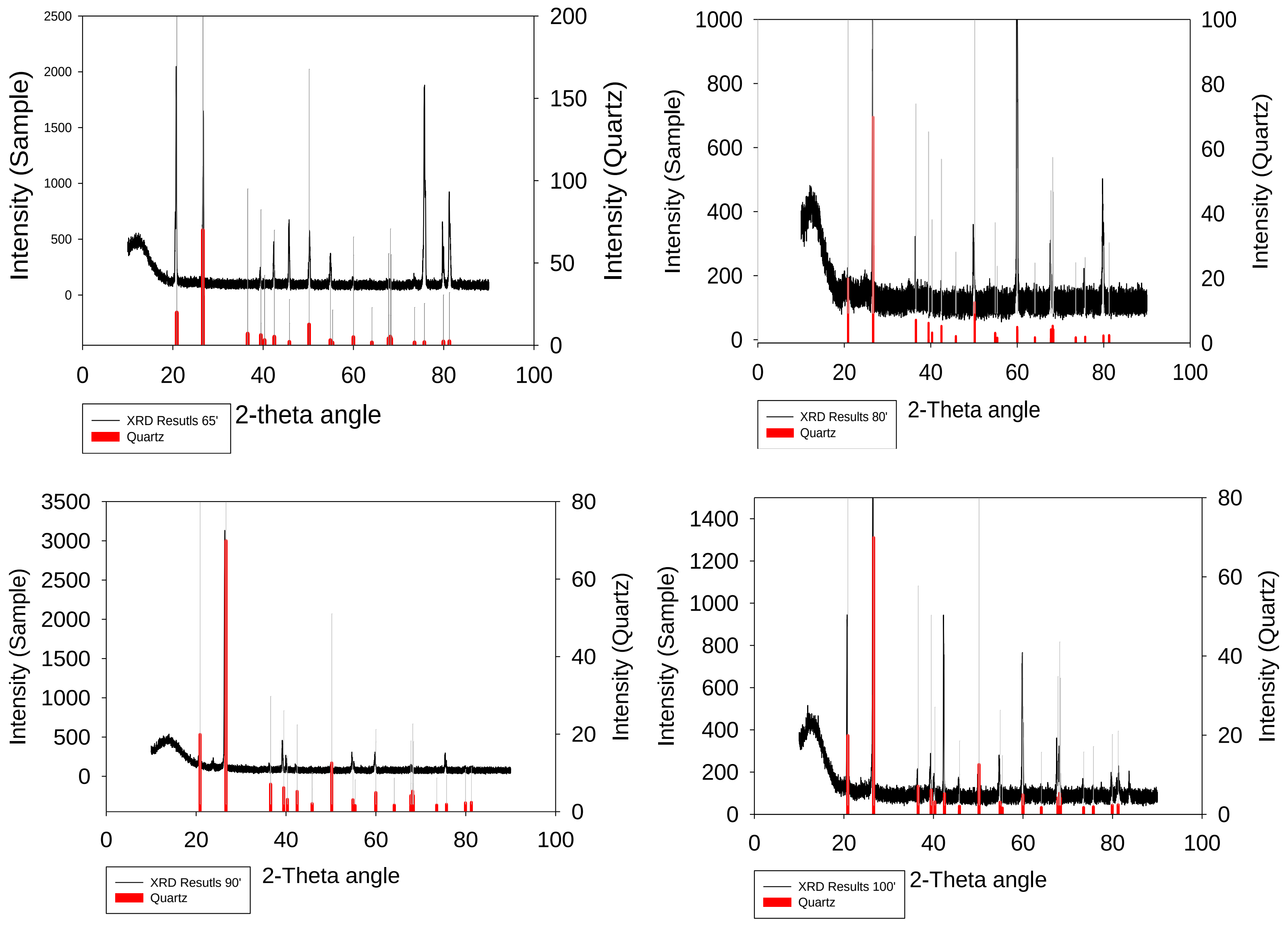

Quartz is the most likely match with 80% of peaks aligning

Future Work ⟶ Re-oxidation

- After six weeks, samples will be sacrificed
- Three types of environments:
  - Anaerobic chamber with no oxygen
  - Small chamber containing 2000 ppm oxygen
  - Work bench at atmospheric oxygen levels
- Sieve samples to analyze fine fractions of less than 0.06 mm

Contact Information

Valentina I. Padilla
10555 West Flagler Street EC 2100
Miami, Florida 33174
vpadilla@fiu.edu

Acknowledgments

Dr. Miles Denham, Dr. Brian Looney, Maggie Milling, Mark Amidon, Dr. Leonel Lagos, and the DOE-FIU Science & Technology Workforce Development Program. This research was supported by U.S. Department of Energy Office Of Environmental Management under grant No. DE-EM0000598.

Rate of Uranium Release from Calcium Meta-Autunite: Effect of Bicarbonate Solutions on the Dissolution - 14218

Ravi K. P. Gudavalli [a],*, Yelena P. Katsenovich [a], Leonel E. Lagos [a], Dawn M. Wellman [b]
[a]Applied Research Center, Florida International University, 10555 W Flagler St., EC 2100, Miami, FL 33174
[b]Pacific Northwest National Laboratory, P.O. Box 999, K3-62, Richland, WA 99352

ABSTRACT

Uranium is a key contaminant of concern at the 300 Area of the Hanford Site that poses risk to humans due to its chemical and radio toxicity. Injection of a soluble sodium polyphosphate amendment into uranium contaminated porous media has been shown to effectively remediate uranium (VI) by forming an insoluble uranyl-phosphate mineral, autunite $X_{1\text{-}2}[(UO_2)(PO_4)]_2 \cdot nH_2O$, where X is monovalent or divalent cations. The release of uranium from calcium meta-autunite occurs during the slow dissolution of the mineral structure. Carbonate is the major ion in the groundwater composition. According to the speciation modeling, uranyl ions (UO_2^{+2}) are predicted to form soluble uranyl-carbonate complexes such as $UO_2(CO_3)_2^{-2}$ and $UO_2(CO_3)_3^{-4}$. Current knowledge on the uranium release from Ca-autunite is limited to the conditions involving pH and temperature; there is a need to assess the effect of bicarbonate on the release of uranium as a result of Ca-autunite mineral dissolution. The rate of uranium release from Ca-autunite in the presence of 0.5-3.0 mM bicarbonate solutions at pH 7-11 and temperature 23-90°C was evaluated via single-pass flow-through (SPFT) experiments. The presence of bicarbonate has been shown to influence the release of uranium from Ca-autunite. At pH 7, the uranium release rate increased 18 times; whereas, at pH 11, the release of uranium was 435 times greater than the release at pH 7. Activation energy values helped identify the rate limiting steps of the dissolution of uranium.

INTRODUCTION

Uranium contamination originated from the discharges at mining and processing sites and is the most common radiological contamination in soil and sediments [1, 13]. Quantitative predictions on the uranium movement in the groundwater are critical for future remediation technologies and disposal of radioactive waste. One of the notable uranium contaminated sites in the United States is the Department of Energy's (DOE) Hanford Site, which contains groundwater plumes contaminated with uranium (VI) that originated from unintended leakages and spills from nuclear production facilities [5]. Activities at the 300 Area of the Hanford Site led to the contamination of streams, soil and groundwater primarily with 58,967 kg of uranium, which poses risks to humans due to its chemical toxicity and risk of radiological exposure. Injection of a soluble sodium polyphosphate amendment into uranium contaminated porous media has been shown to effectively remediate uranium by forming an insoluble uranyl-phosphate mineral, autunite $X_{1\text{-}2}[(UO_2)(PO_4)]_{2\text{-}1} \cdot nH_2O$, where X is monovalent or divalent cations [16, 17, 19, 20]. Calcium is the most abundant metal in the earth's crust and, in Ca- rich environments typical for the western US, Ca replaces Na and the exchange takes place rapidly into Ca-autunite. Carbonate is the major ion in the groundwater composition at the 300 Area of the Hanford Site. According to the speciation modeling, uranyl ions (UO_2^{+2}) are predicted to form soluble uranyl-carbonate complexes such as $UO_2(CO_3)_2^{-2}$ and $UO_2(CO_3)_3^{-4}$ [19]. Current knowledge on the uranium release from Ca-autunite is limited to the conditions involving pH and temperature; there is a need to assess the effect of bicarbonate on the release of uranium as a result of Ca-autunite mineral dissolution. The objective of this research was to quantify the effect of bicarbonate solutions (0.5-3.0 mM) on the rate of uranium release at varying pH (7-11) and temperature (23-90^{o}C) conditions.

MATERIALS AND METHODS

Autunite Specimens

The natural Ca-autunite, $Ca[(UO_2)(PO_4)]_2 \bullet 3H_2O$, used in the experiments was obtained from Excalibur Mineral Corporation (Peekskill, New York). The autunite mineral was previously characterized by Wellman et al. (2006) by using ICP-OES, ICP-MS analyses, X-ray diffraction and SEM/EDS and confirmed to be 98-99% pure autunite. The autunite sample was powdered to have a size fraction of 75 to 150 μm (-100 to +200 mesh) with an average surface area of 0.88 m^2 g^{-1}.

Single-Pass Flow-Through (SPFT) Experiments

Dissolution of minerals is a complex process that involves a series of reactions occurring at the mineral-water interface. The dissolution process is also dependent on the rate limiting reaction [12, 13, 15]. Transition state theory (TST) is widely applied to estimate the reaction rates of elementary reactions. TST is based on the assumption that the dissolution is controlled by the desorption kinetics of an activated complex formed at the surface of a solid phase. A general form of the TST rate equation is centered on the prediction that the overall reaction rate is governed by the slowest elementary reaction, known as the rate-limiting step [11]. The reaction is given by

$$r = k\, v_i\, a_{H^+}^{\pm\eta} \exp\left(\frac{-E_a}{RT}\right)\left[1-\frac{Q}{K_g}\right]^{\sigma} \prod_j a_j^{n_i}, i = 1,2,....N \qquad \text{(Eq. 1)}$$

Where:

r = dissolution rate in g m^{-2} d^{-1},

k = intrinsic rate constant in g m^{-2} d^{-1},

v_i = mass fraction of element i,

a_j = activity of the j^{th} aqueous species that acts as an inhibitor or catalyst,

E_a = activation energy in kJ mol^{-1},

R = gas constant in kJ mol^{-1} K^{-1},

T = temperature in ^{o}K,

Q = ion activity product,

K_g = pseudo equilibrium constant,

η = power law coefficient, and

σ = Temkin coefficient.

The Ca-autunite dissolution rate was measured via single-pass flow-through (SPFT) experiments at varying concentrations of bicarbonate (0.5 - 3.0 mM) in a pH range of 7 to 11 and temperature range of 23^{o} to 90^{o}C (Fig. 1). SPFT experiments are designed to measure reaction rates at the forward rate under tightly controlled conditions.

Fresh buffer solutions prepared with distilled, de-ionized water (DDIW) with 0.5 - 3.0 mM bicarbonate solutions buffered with 0.01 M *tris (hydroxymethyl) aminomethane* (TRIS) were used to investigate U(VI) release from a natural Ca-autunite mineral. Concentrated trace-metal grade nitric acid and lithium hydroxide were used to adjust the pH of buffer solutions in the range of 7-11. A 0.25 g sample of powered Ca-autunite was introduced into the reactor that came into contact with the buffered bicarbonate solutions. The effluent solutions from the SPFT reactor cells were continuously collected until steady state conditions were achieved. Effluent solutions were wet- and dry-ashed to reduce the interference of organic content on the analytical instruments. Dissolved concentrations of U(VI) were quantified using kinetic phosphorescence analyzer (KPA-11) and Ca and P concentrations were analyzed by means of ICP-OES (Optima 7300).

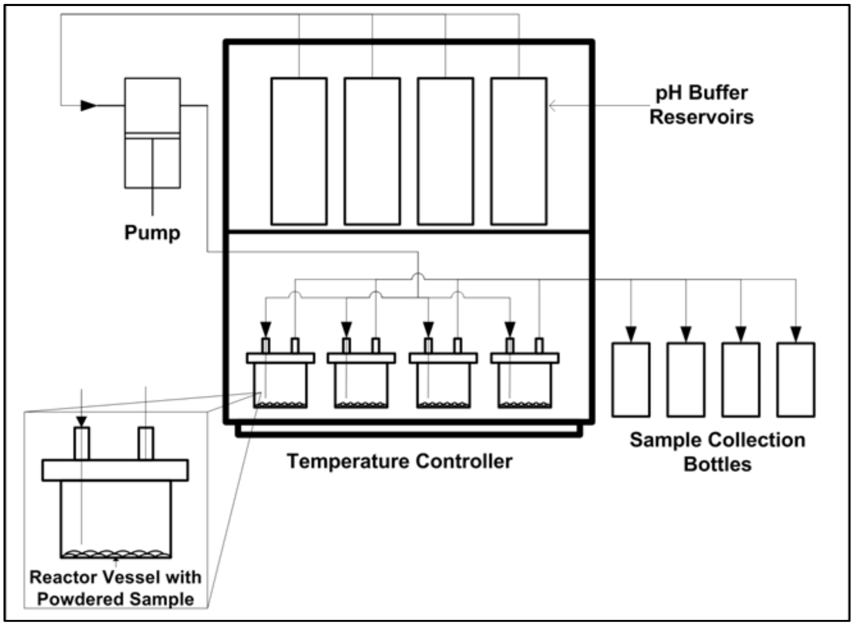

Fig. 1. Experimental Setup With Single-Pass Flow-Through Apparatus

Quantification of Dissolution Rate

The normalized dissolution rate of Ca-autunite solids was calculated from Eq. 2 when the system reached equilibrium [11].

$$R_i = (C_i - C_{ib})\frac{q}{f_i S} \qquad \text{(Eq. 2)}$$

Where:

R_i = normalized dissolution rate for element *i* (mol m^{-2} s^{-1}),

q = flow rate (L d^{-1}),

C_i = concentration of component *i* in the effluent (g L^{-1}),

C_{ib} = mean background concentration of component *i* (g L^{-1}),

f_i = mass fraction of the element in the metal (dimensionless), and

S = surface area of the sample (m^2).

The steady-state conditions were achieved after approximately eight reactor volumes were exchanged and the concentrations of uranium released from natural Ca-autunite became invariant with respect to time for all pH and bicarbonate ranges tested.

The standard deviation of the dissolution rate was determined according to the uncertainty associated with each parameter shown in Equation 2. Standard deviation for uncorrelated random errors is given by:

$$\sigma_f = \sqrt{\sum_{i=1}^{n}\left(\frac{\partial f}{\partial x_i}\right)^2 \sigma_i^2} \qquad \text{(Eq. 3)}$$

Where: σ_f - standard deviation of the function f ; x_i - parameter i; and σ_i -standard deviation of parameter i.

Substituting Eq. 2 in Eq. 3 and converting to relative standard deviation 2, $\hat{\sigma}_r = {}^{\sigma_f}\!/_{\bar{x}}$, yields

$$\hat{\sigma}_r = \sqrt{\frac{\left(\hat{\sigma}_c C_i^{out}\right)^2 + \left(\hat{\sigma}_b C_i^{in}\right)}{\left(c_i^{out} + c_i^{in}\right)^2} + \hat{\sigma}_{fi}^2 + \hat{\sigma}_s^2 + \hat{\sigma}_q^2} \qquad \text{(Eq. 4)}$$

Uncertainty associated with each parameter was considered when calculating the dissolution rate; relative errors included are final concentration (10%), background concentration (10%), mass distribution (5%), surface area (15%), and flow rate (5%). This error analysis results in typical 2σ uncertainties of approximately ±35% for SPFT-measured dissolution rates (or ±0.2 log units when reported as log10 rates) [17]. The experimental results were correlated by linear regression using SigmaPlot-11.2 (Systat Software Inc.).

Groundwater Modeling

Steady state elemental concentrations in the effluent solution after the system reached equilibrium were used to identify the predominant uranium species in the aqueous solution. The speciation modeling was performed by means of geochemical modeling software Visual MINTEQ v. 3.0, maintained by J. Gustafsson at KTH, Sweden, available at http://www.lwr.kth.se/English/OurSoftware/vminteq/ using thermodynamic data from Grenthe et al, (1992) and updated with the Nuclear Energy Agency's thermodynamic database for uranium (Guillaumont et al., 2003), calcium-uranyl-carbonate complexes (Dong and Brooks, 2006), and becquerelite dissolution data by Gorman-Lewis et al. (2008). The uranium speciation and solubility calculations are based on current knowledge and may have significant associated uncertainties.

RESULTS AND DISCUSSION

Influence of bicarbonate

The influence of bicarbonate on the dissolution of Ca-autunite was experimentally determined using Eq. 5:

$$\log(r) = \log(k) + \eta \log\left[HCO_3^-\right] \qquad \text{(Eq. 5)}$$

Where:

r = dissolution rate (mol m^{-2} s^{-1}),

k = intrinsic rate constant (mol m^{-2} s^{-1}), and

$[HCO_3^-]$ = concentration of pH-adjusted bicarboante solutions (mol L^{-1}).

A non-linear regression was performed for each temperature with dissolution rates as a function of the concentration of the bicarbonate solutions to determine slope and the power law coefficient, η. The resulting regression coefficient over the entire data helped to define the intrinsic rate constant, *k* (mol m^{-2} s^{-1}).

Data presented in Fig. 2 shows the change in the rate of release of uranium from Ca-autunite with the change in bicarbonate concentrations tested and the temperature range of 23 - 90 °C. A strong influence of pH was displayed on the release of uranium from Ca-autunite which is in agreement with the results previously reported [16, 17]. An approximate 18-fold increase in the rate of uranium release was observed with an increase in the bicarbonate concentration from 0.5 to 3.0 mM; the resulting regression coefficients are η = 0.50 ± 0.12 and k = 1.09 × 10^{-09} (mol m^{-2} s^{-1}). The influence of bicarbonate concentration on the release of uranium from Ca-autunite was shown to increase with an increase in pH. At pH 8 - 11, the increase in the uranium release were 17, 65, 392 and 434 fold at pH 8, 9, 10 and 11, respectively, when compared to the values at pH 7. The values of the power law coefficient and the intrinsic rate constants at pH 7 - 11 are shown in TABLE I.

TABLE I Experimentally determined data for Ca-autunite dissolution

pH	Ca-autunite			
	η	k (mol m^{-2} s^{-1})	K_g	ΔH (kJ mol^{-1})
7	0.50 ± 0.12	1.09 x 10^{-09}	0.65	28.58
8	0.52 ± 0.10	3.15 x 10^{-09}	0.79	11.83
9	0.79 ± 0.08	5.60 x 10^{-08}	4.20	11.90
10	1.09 ± 0.11	1.58 x 10^{-06}	25.97	15.88
11	0.94 ± 0.06	6.99 x 10^{-07}	27.75	13.84

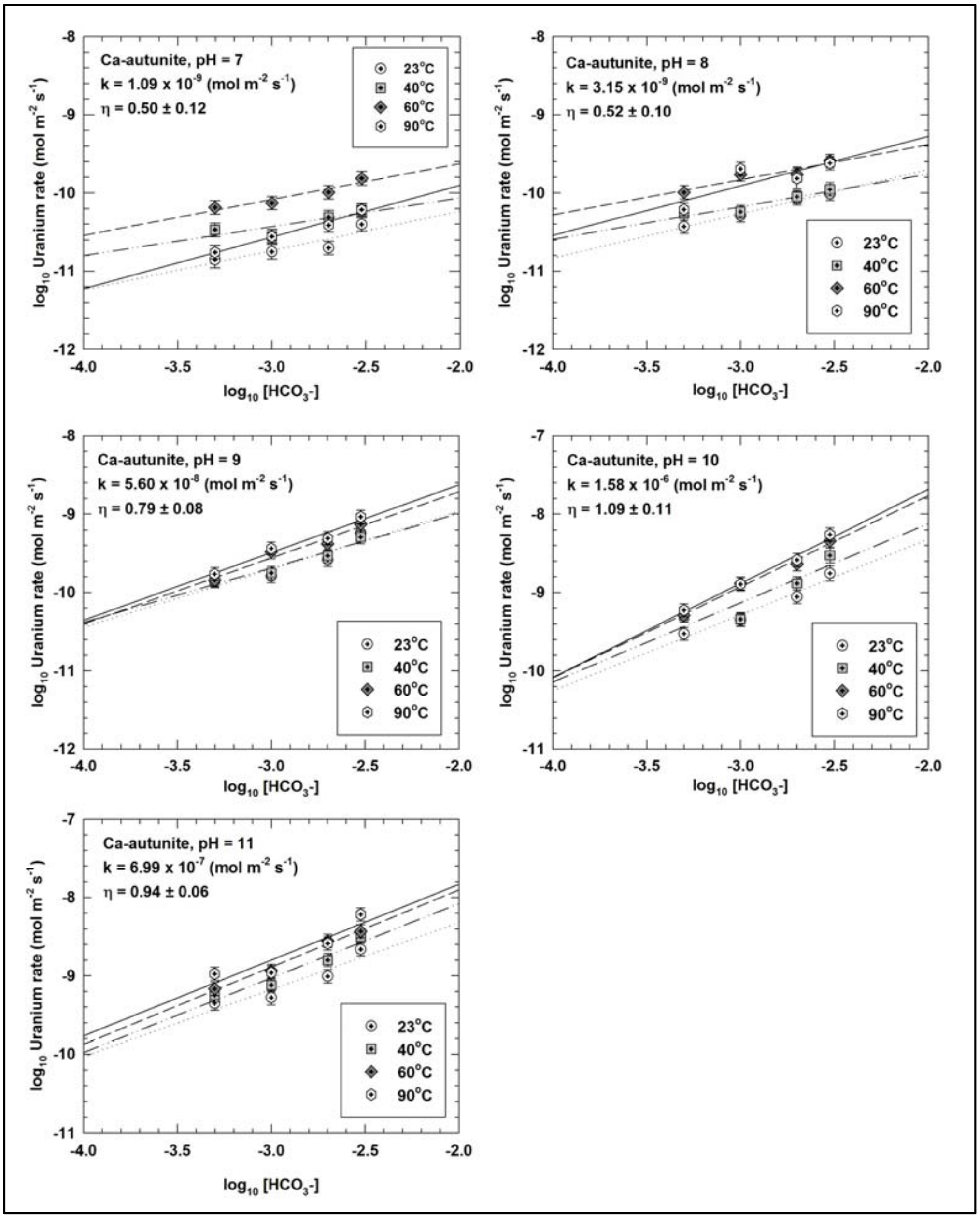

Fig. 2. Uranium Release Rate With The Change In Bicarobnate Concentrations At pH 7-11

At pH 7, the geochemical modeling data indicated that the possible uranyl secondary phase minerals (beta-$UO_2(OH)_2$ and schoepite) are under-saturated, suggesting that the release of U(VI) is solely due to the dissolution of Ca-autunite. At pH 8 and 9, the increase in aqueous bicarbonate concentrations correlated with a decrease in the saturation indices of potential secondary phases as schoepite and β-$UO_2(OH)_2$, suggesting a faster release of U(VI) from autunite under these conditions. At pH 9-11, hydroxyapatite became supersaturated at all bicarbonate concentrations along with other secondary Ca-P minerals controlling the net release of uranium. The increase in the uranium release rate with increasing pH could be explained by the increase in CO_3^{2-} as the distribution of dissolved inorganic carbon depends on pH. The increased availability of CO_3^{2-} helped to form strong and highly soluble uranyl-carbonate and calcium-uranyl-carbonate complexes.

The predominant uranyl species at all pHs tested was $UO_2(CO_3)_3^{-4}$, accounting for approximately 70% of the total uranyl species. $H_2PO_4^{-2}$ was the major phosphate species, accounting for nearly 60% at all pH conditions tested. Calcium species distribution showed the dependency on pH. At pH 7, the system was dominated by Ca^{2+} ions while the $CaUO_2(CO_3)_3^{-2}$ species became predominate at pH 8 to 10, representing approximately 95% and 80% of the total Ca species, respectively. At pH 11, 85% of Ca was found in the form of $CaPO_4$. Based on the information obtained from the Visual MINTEQ geochemical modeling software, the following elementary reactions are proposed for dissolution reactions at pH 7-10 (Eq. 6) and pH 11 (Eq. 7):

$$Ca\left[(UO_2)(PO_4)\right]_2 xH_2O + HCO_3^- \rightarrow UO_2\left(CO_3\right)_3^{-4} + Ca\left(UO_2\right)\left(CO_3\right)_3^{-2} + HPO_4^{-2} + Ca^{+2} + xH_2O \tag{Eq. 6}$$

$$Ca\left[(UO_2)(PO_4)\right]_2 xH_2O + CO_3^- \rightarrow UO_2\left(CO_3\right)_3^{-4} + HPO_4^{-2} + CaPO_4^- + xH_2O \tag{Eq. 7}$$

The release of uranium from an autunite mineral is a surface mediated reaction that occurs in several steps [12, 15]. It starts with the fast attachment of a reactant to the surface of the mineral through the surface cracks, followed by the rate-limiting detachment of metal species from the surface. The release of uranium from autunite mineral under the influence of bicarbonate is expected to take place via a two-step process of surface coordination of bicarbonate/carbonate ion followed by the detachment of uranyl carbonate/calcium uranyl carbonate.

Activation energy, E_a, is a unique parameter that describes the nature of the reaction; faster reactions have small activation energy values and slower reactions have higher activation energy values. Zhang et al. (2001) previously reported that pH has a noticeable influence on the activation energy. Also activation energy values help to identify the rate-controlling process of the dissolution of minerals [1, 10]. Reactions with activation energy values less than 20 kJ mol^{-1} are often indicative of surface diffusion rate-controlling reactions. Surface controlled dissolution usually results in higher activation energy.

A modified transition state theory equation describing the rate of reaction as a function of temperature and the activities of the rate enhancing or inhibiting species were used to estimate the activation energy values, described as:

$$r = k\, e^{\frac{-E_a}{RT}} \left[HCO_3^-\right]^{\eta} \tag{Eq. 8}$$

Where:

r = dissolution rate (mol m^{-2} s^{-1}) experimentally determined from SPTF tests,

k = intrinsic rate constant (mol m^{-2} s^{-1}),

$[HCO_3^-]$ = concentration of bicarbonate solutions (mol L^{-1}),

η = power law coefficient (dimensionless),

E_a = activation energy (J mol^{-1}),

R = universal gas constant (J mol^{-1} K^{-1}), and

T = temperature (^{o}K).

Fig. 3 depicts normal logarithmic values of the rate of dissolution (ln r) plotted against the values of inverse temperature (T^{-1}) at a constant bicarbonate concentration and at different pH values. The slope of the regression line at each bicarbonate concentration represents activation energy values, which were further averaged at each pH (Table II). The close proximity of regression lines is indicative of the weak effect of HCO_3^- solutions on the rate of uranium release at pH 7 and 8, whereas the separation of curves at pH 9-11 is an indication of rapid uranium release when the concentration of CO_3^{2-} became prominent.

Table II activation energy values of Ca-autunite dissolution at various pH

$[HCO_3^-]$ (M)	Ca-autunite			
	0.0005	0.001	0.002	0.003
pH	E_a (kJ mol^{-1})			
7	21.87	26.39	27.72	26.00
8	22.41	20.72	15.57	13.95
9	2.63	13.07	8.95	7.32
10	8.17	16.68	15.05	15.17
11	11.39	10.19	12.23	11.78

The average activation energy at pH 7 for Ca-autunite was estimated to be 25.50 kJ mol^{-1} and the average activation energy at pH 8 -11 was in the range of 8-18 kJ mol^{-1}. Activation energy at pH 7 is an indication that the dissolution is controlled by the surface bond-breaking of uranyl carbonate and calcium uranyl carbonate ions occurring at the solid/liquid interface by which surface-bound ions move into solution. At pH 8 and above, the reaction is controlled by the rate-limiting mass transfer step of the reaction leading to the crystal sheets cracking or splitting apart.

The pseudo equilibrium constant and the enthalpy of the system were estimated using Eq. 9 and Eq 10. Equation 9 was obtained based on the assumption that the rate limiting factor is the concentration of bicarbonate solutions [8].

$$r = K_g\left[HCO_3^-\right] \qquad \text{(Eq. 9)}$$

$$\Delta\mathrm{H} = -RT\ \ln K_g \qquad \text{(Eq. 10)}$$

Where:

r = dissolution rate (g m^{-2} d^{-1}) experimentally determined from SPTF tests,

$[HCO_3^-]$ = concentration of bicarbonate solutions (mol L^{-1}),

ΔH = enthalpy (J mol^{-1}),

R = universal gas constant (J mol^{-1} K^{-1}), and

T = temperature (^oK).

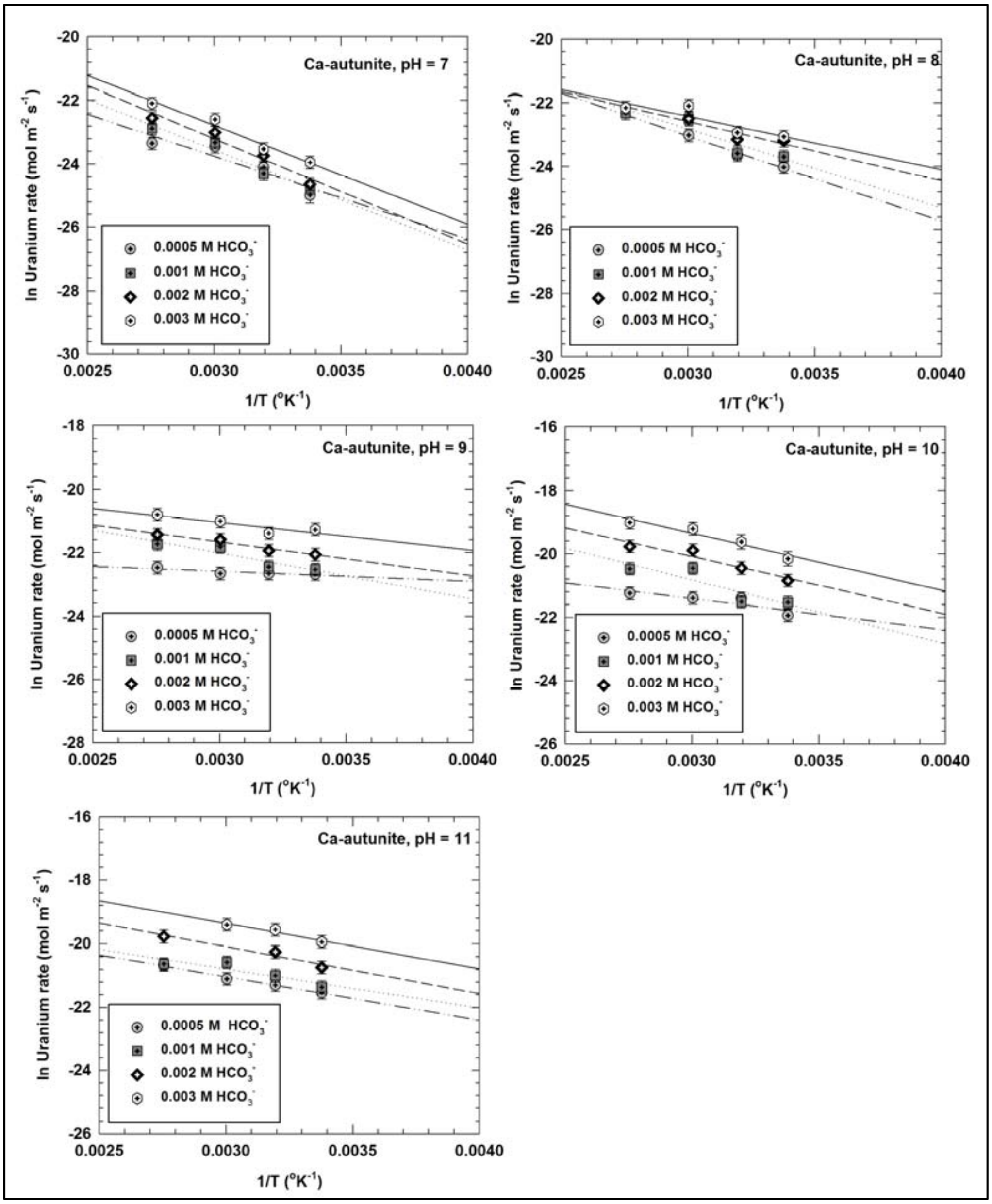

Fig. 3. Change in the ln of Uranium Release Rate from Ca-Autunite versus Values of Inverse Temperature

The change in the uranium release rate against the change in the bicarbonate concentration were plotted at different pH values and the slope of the regression lines provided the values of the pseudo equilibrium constant (Fig. 4 and TABLE I). This data suggests that the reaction occurred slowly at low pH values and significantly faster at high pH values. A similar trend was shown by the intrinsic rate constant values. A slope of a linear graph with inverse temperature (T^{-1}) on the X-axis and the normal logarithmic values of the pseudo equilibrium constant, ln K_g, on the Y-axis (Fig. 5) were used to estimate the enthalpy of the system at various pH values (TABLE I). This change might not be significant enough to justify any principal differences in the uranium release reaction mechanisms; however, it correlates with the trend shown by the intrinsic rate constant pertaining to Ca-autunite dissolution suggesting higher U release from this phase.

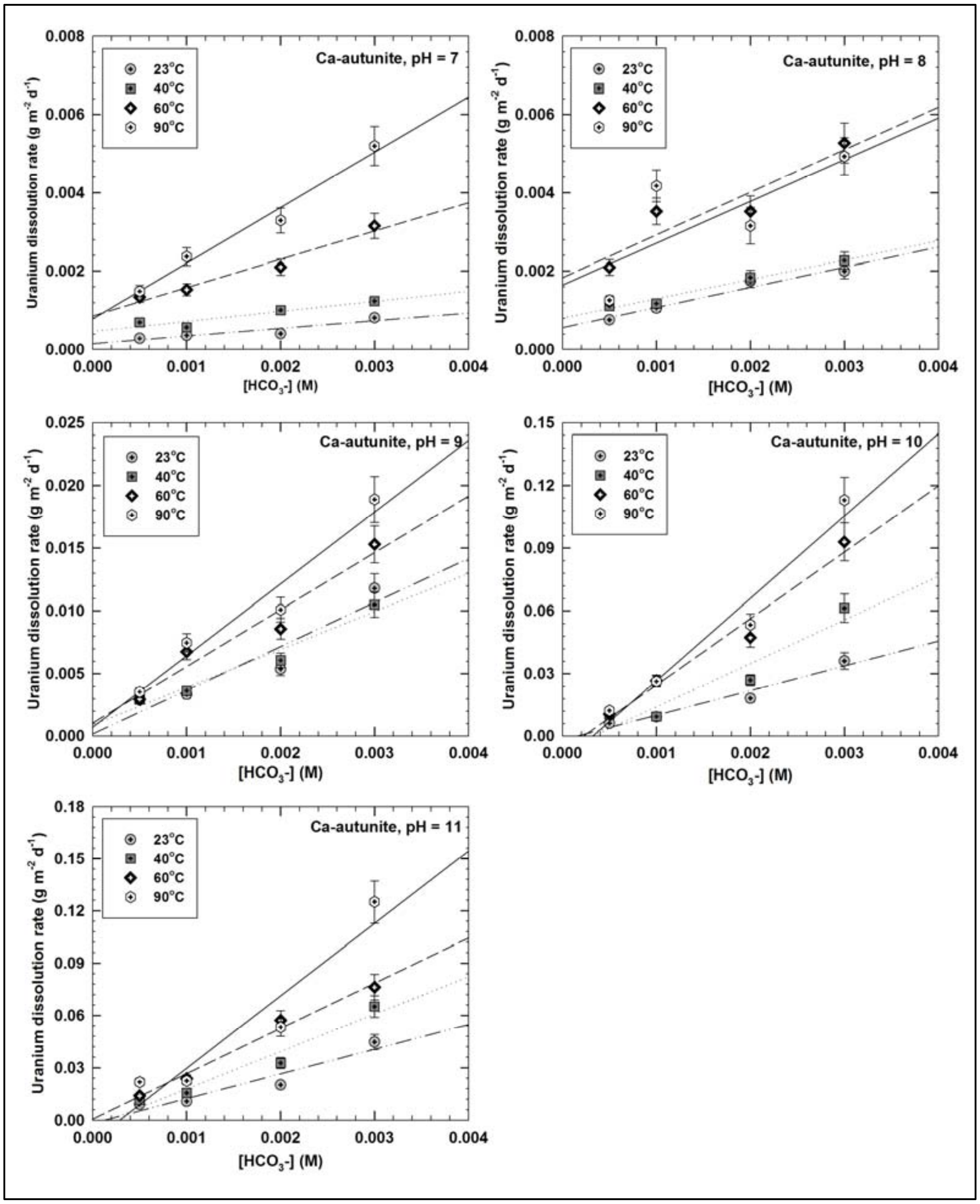

Fig. 4. Uranium Release Rate as a Function of Bicarbonate Solution Concentrations at Various pH Values

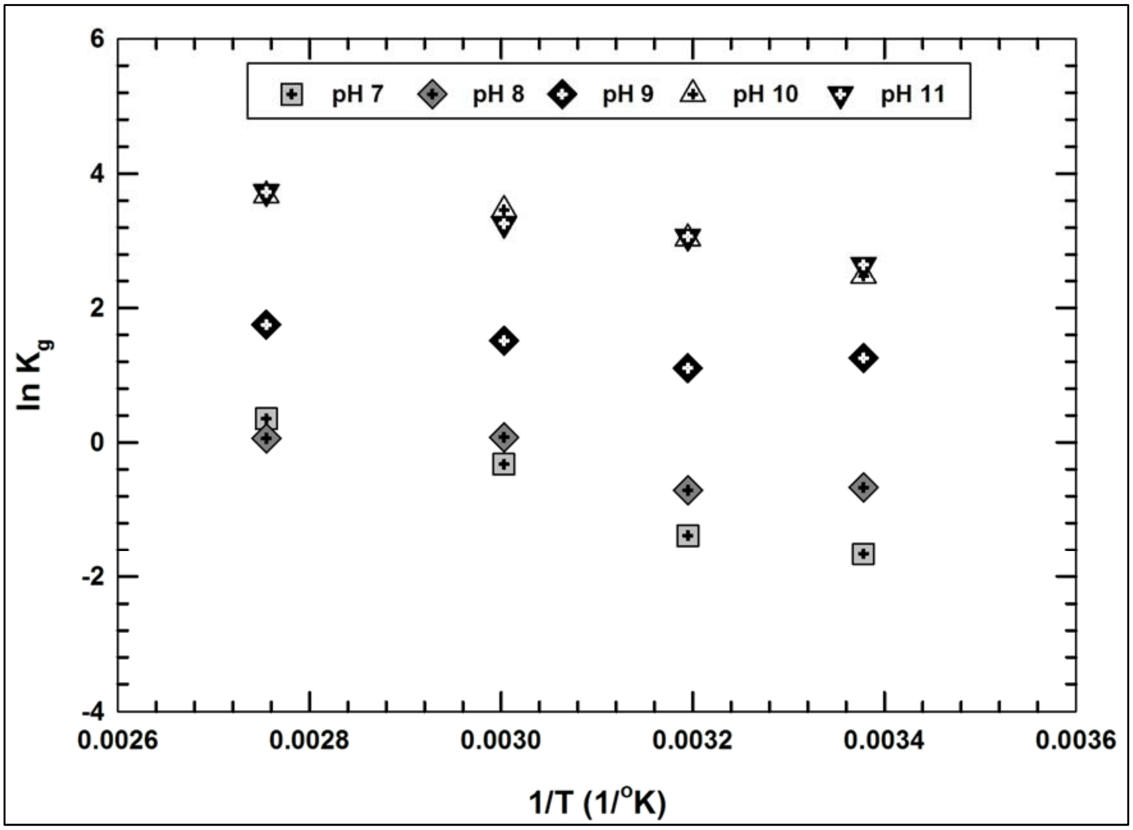

Fig. 5. Changes in the Pseudo Equilibrium Constant as a Function of Inverse Temperature

CONCLUSIONS

The rate of uranium release from the Ca-autunite under the bicarbonate concentration ranging from 0.5 - 3.0 mM, and at pH 7-11 and temperature of 23 - 90 °C was investigated via single-pass flow-through apparatus. The power law coefficient, η, was found to be between 0.5 and 1.0, with no finite temperature dependency on the uranium release. Pseudo equilibrium and enthalpy data showed that the dissolution process is slower at pH 7; at pH 8 and beyond the speed of dissolution increased. A similar observation was made based on the activation energy values; at pH 7, elevated activation energy suggested that the reaction is deliberate and at pH values 8-11, activation was low, suggesting a faster reaction. The dissolution rate data indicates that low concentrations of bicarbonate in the subsurface environment can impact the stability of the uranyl phosphate minerals. The information presented here provides critical fundamental aspects to refine the bulk kinetic parameters currently being used to predict the stability of autunite minerals and the fate of uranium in the subsurface.

REFERENCES

1. Bemer R. A., 1978. Rate control of mineral dissolution under earth surface conditions. Am. J. Sci. 278, 1235-1252.
2. Bernhard G., Geipel. G., Reich, T., Brendler, V., Amayri, S., Nitsche, H. Uranyl(VI) Carbonate Complex Formation: Validation of the Ca2UO2(CO3)3(aq.) Species [Journal]. - Germany: Radiochim. Acta, 2001. - Vol. 89. - pp. 511-518.
3. Dong, W. and S. C. Brooks. 2006. Determination of the formation constants of ternary complexes of uranyl and carbonate with alkaline earth metals ($Mg^{2+,}$ Ca^{2+}, Sr^{2+}, and

Ba^{2+}) using anion exchange method. Environ. Sci. Technol. 40(15):4689-4695. doi: 10.1021/es0606327.

4. Elias D.A., Senko, J.M., Krumholz, L.R. A Procedure for Quantification of Total Oxidized Uranium for Bioremediation Studies: Journal of Microbiological Methods, 2003, Vol. 53, pp. 343-353.
5. Elless M.P., Lee, S.Y. Uranium solubility of carbonate-rich-uranium-contaminated soils. Water, Air, and Soil Pollution, 1998, pp. 147-162.
6. Gorman-Lewis D., Fein JB., Burns PC., Szymanowski J.S., Converse J., 2008. Solubility measurements of the uranyl oxide hydrate phases metaschoepite, compreignacite, Na-compreignacite, becquerelite, and clarkeite. J. Chem. Thermodyn. 40, 980 -990.
7. Grenthe I., Fuger J., Konings R. J. M., Lemire R. J., Muller A. J., Nguyen-Trung C., Wanner H., 1992. Chemical Thermodynamics of Uranium. Elsevier, Amsterdam.
8. Gudavalli R., 2012. Effect of pH and temperature on the carbonate promoted dissolution of sodium meta-autunite. Ph.D. dissertation, Florida International University Miami, FL.
9. Guillaumont R., Fanghänel T., Fuger J., Grenthe I., Neck V., Palmer D.A., Rand M.H., 2003. Chemical Thermodynamics, OECD Nuclear Energy Agency vol. 5, Elsevier, 919 pp.
10. Jordan G., Rammensee W., 1996. Dissolution rates and activation energy for dissolution of brucite (001): A new method based on the microtopography of crystal surfaces. Geochim. Cosmochim. Acta, 60(24), p 5055-5062.
11. McGrail B. P., Ebert W. L., Bakel A. J., Peeler D. K., 1997. Measurement of kinetic rate law parameters on a Na- Ca- Al borosilicate glass for low-activity waste. J. Nucl. Mater., 249 (2), 175-189.
12. Nagy K.L., 1995. Dissolution and precipitation kinetics of sheet silicates. In A.F.White and S.L. Brantley (eds): Chemical Weathering Rates of Silicate Minerals, pp. 173-233, Mineralogical Society of America, Washington, D. C.
13. Pablo J. D., Casas I., Gimenez J., Molera M., Rovira M., Duro L., 1999. The oxidative dissolution mechanism of uranium dioxide. I. The effect of temperature in hydrogen carbonate medium. Geochem. Cosmochim. Acta, 63, 3097-3103.
14. Riley R.G., Zachara J.M., Wobber F.J., 1992. Chemical Contaminants on DOE Lands and Selection of Contaminant Mixtures for Subsurface Science Research. - Washington. DC : U.S. Department of Energy, Office of Energy Research.
15. Sparks D. L., 1999. Kinetics and Mechanisms of Chemical Reactions at the Soil Mineral/Water Interface. Soil Physical Chemistry. 2nd ed. CRC Press LLC.
16. Wellman D.M., Gunderson, K.M., Icenhower, J.I., and Forrester, S.W. // Dissolution kinetics of synthetic and natural meta-autunite minerals, X3-n n+[(UO2)(PO4)]2 XH2O, under acidic conditions. Geochemistry Geophysics Geosystems, 2007.
17. Wellman D.M., Icenhower, J.P., Gamerdinger, A.P., Forrester, S.W. Effects of pH, temperature, and aqueous organic material on the dissolution kinetics of meta-autunite minerals, (Na, Ca)2-1[(UO2)(PO4)]2 3H2O. American Mineralogist, 2006, pp. 143-158.
18. Wellman D.M., McNamara, B.K., Bacon, D.H., Cordova, E.A., Ermi, R.M., Top, L.M. Dissolution kinetics of meta-torbernite under circum-neutral to alkaline conditions. Environmental Chemistry, 2009, pp. 551-560.
19. Wellman D.M., Pierce, E.M., Richard, E.L., Fruchter, J.S., Vermuel, V.R., Uranium Plume Treatability Demonstration at the Hanford Site 300-Area: Development of Polyphosphate Remediation Technology for In Situ Stabilization of Uranium. Phoenix, AZ. WM2008.
20. Zachara J.M., Davis, J.A., McKinley, J.P., Wellman, D.M., Liu, C., Qafoku, N., Yabusaki, S.B. Uranium Geochemistry in Vadose Zone and Aquifer Sediments from the 300 Area Uranium Plume [Report]. Prepared for the U.S. Department of Energy under contract DE-AC05-76RL01830: PNNL-15121, 2005.

21. Zhang Y., Hart K.P., Bourcier W.L., Day R. A., Colella M., Thomas B., Aly Z., Jostsons A., 2001. Kinetics of uranium release from Synroc phases, J. Nucl. Mater. 289 (3), p. 254-262.

ACKNOWLEDGEMENTS

Funding for this work was provided by the U.S. Department of Energy Office of Environmental Management under grant DE-EM0000598. This manuscript was prepared in collaboration with the Deep Vadose Zone- Applied Field Research Initiative at Pacific Northwest National Laboratory. The Pacific Northwest National Laboratory is operated by Battelle Memorial Institute for the Department of Energy (DOE) under Contract DE-AC05-76RL01830. We gratefully acknowledge the efforts of A. Henao for his assistance in conducting KPA and ICP-OES analysis.

The Effect of Ca Ions on the Removal of U(VI) via *In-Situ* Ammonia Gas Injection at the Hanford Site 200 Area-14434

Yelena Katsenovich, Claudia Cardona, Leonel Lagos
Applied Research Center, Florida International University, 10555 W Flagler St., EC 2100,
Miami, FL 33174

ABSTRACT

This study investigates the mechanisms and effectiveness of U removal from the solution mixture replicating the pore water composition found at the Hanford Site vadose zone (VZ). A series of batch experiments were conducted to evaluate the effect of Ca concentrations at various molar ratios of silicon to aluminum, in the presence of several bicarbonate concentrations on the removal of U(VI) and other elements. Evidently, an understanding of the role of pore water constituencies on the removal of U(VI) is needed to predict the mineralogical changes and the formation of precipitates that would be created in the treated VZ soil. For the initial experiments, the complicated pore water composition was simplified to have only five major components in the test solutions: uranium, silica, aluminum, bicarbonate and Ca. The tests were carried out with varied Si concentrations to study different Si:Al molar ratios. The Al concentration was kept constant at 5 mM and bicarbonate concentrations varied between 0 and 100 mM. To evaluate the effect of Ca, the water composition included 5 mM or 10 mM of Ca ions.

The results indicated that the percentage of U(VI) removal was largely controlled by the Si/Al ratios and calcium concentrations. The percent of U(VI) removal increased as Si/Al ratios and calcium concentrations were increased. The higher Ca concentration correlated with higher U(VI) removal, ranging between 96%-99%, at low Si/Al ratios between 1 and 10. It was clear that the increase in Ca concentration correlated with higher removal of Si from the solution mixture. When the Ca concentration was increased up to 10 mM, the percentage of silica removal at Si:Al ratio 1, the lowest ratio investigated in this study, was increased to 93-99%. In all of the experiments, the removal of Si correlated with the removal of U(VI) from solutions. If the supernatant solutions showed a small decline in Si concentrations, the removal in U(VI) was diminutive or not observed. The results suggest the effectiveness for the potential implementation of NH3 gas injection for the remediation of the U(VI)-contaminated VZ.

INTRODUCTION

Past uranium-plutonium extraction and enrichment processes at the Hanford Site 200 Area have left approximately 200,000 kg of legacy uranium contamination in the vadose zone (VZ). This uranium is a potential source for groundwater contamination and a risk to receptors through water uptake from contaminated wells or discharges to surface water. Despite extensive remediation efforts initiated in the early 1990s, uranium groundwater plumes identified in multiple locations around the site have persisted for many years. Uranium is present in the VZ sediment as uranyl-carbonates (liebigite and rutherfordine), co-precipitated with carbonates and hydrous silicates and Na-boltwoodite. The dominate uranium species are stable ternary calcium-uranyl-carbonate complexes, $UO_2CO_3^0$, $UO_2(CO_3)_2^{2-}$ and $UO_2(CO_3)_3^{4-}$, which are highly soluble and, therefore, mobile under VZ oxidizing conditions [1, 2].

The injection of gases is simple and inexpensive method for in situ treatment of heavy metals and radionuclide contamination, which commonly resides in the vadose zone. This method is more efficient and predictable than injection of liquid or solid reagents since gas can more effectively penetrate low permeability soil and sediments [3]. The injection of reactive gases, such as ammonia gas (NH_3), is a novel technology to effectively mitigate uranium contamination in the VZ and reduce the potential for radionuclide mobility in the subsurface. This technology is able to decrease the mobility of uranium species without water addition causing undesired downward contaminant migration. The VZ at Hanford 200 area is deep, having depths between about 150 and 200 feet (46m-61m), and composed of sediments such as quartz, plagioclase, orthoclase, muscovite, biotite, hornooblende, illite, calcite, montmorillonite, chlorite, kaolinite, smectite and kaolinite [4]. All of these minerals may undergo dissolution reactions in the hyperalkaline conditions increasing elemental concentrations in porewater.

NH_3 is a highly soluble gas and its injection in the VZ causes the formation of ammonia hydroxide (NH_4OH) and a subsequent increase in pH. The NH_3 gas rapid partition into liquid results in the aqueous speciation reactions written as [4]:

$$NH_3\ (g) \leftrightarrow NH_3\ (aq) \quad K_h = 6.58 * 10^{-4}\ N \qquad [Eq.1]$$

$$NH_3\ (aq) + H^+ \leftrightarrow NH_4^+,\ pK = 9.4 \qquad [Eq.2]$$

Where K_h is the dimensionless Henry's Law partition coefficient and pK is the negative logarithm of the dissociation constant.

The alkaline conditions can greatly enhance the solubility rates of most Si-containing soil minerals such as feldspar and quartz present in the Hanford Site vadose zone. Chou and Wollast (1984[5]) previously illustrated that the rate of feldspar dissolution has been shown to increase by two to three orders of magnitude with an increase in pH from 8 to 12 at 23ºC. These dissolution reactions potentially induce the release of cations such as Si, Al, Ca, Mg, Na, and K from soil minerals to pore water. The following decrease in pH as the system stabilizes and reaches natural equilibrium will cause uranium co-precipitation during the recrystallization of minerals. Szecsody et al, (2010b [6]) hypothesized that under alkaline conditions aluminosilicates originated from the dissolution of some specific clays might precipitate and coat surface of U-bearing phases. There is a need for a better understanding of the effects of pore water constituencies on the U co-precipitation process. Previous short-term laboratory evaluation showed a decrease in U mobility after ammonia gas injection in the low water content sediments [7]. This technology has significant uncertainty under the 200 Area VZ specific conditions and requires additional testing in the laboratory to understand the effect of various environmental factors on the formation and precipitation of uranium-bearing solid phases. Particularly, what requires clarification is the role of major pore water constituents on the removal of uranium and the formation of precipitates after the NH_3 injection. This investigation is focusing on the effect of concentration ratios of silicon to aluminum, in the presence of various bicarbonate and calcium concentrations, on the removal of U(VI) under conditions imitating the pore water composition of the Hanford Site 200 Area vadose zone.

MATERIAL AND METHODS

The composition of borehole 299-E33-45 pore water has been previously characterized for major cations (Ca^{2+}, Na^+, K^+, Mg^{2+}, Fe^{2+}, Al^{3+}, and Si^{4+}), anions (F^-, Cl^-, NO_2^-, Br^-, SO_4^-, NO_3^-), and pH [8]. In the test solutions used for these experiments, the pore water composition was simplified to contain only five elements such as silica, aluminum, uranium, bicarbonate and calcium. Previous studies confirmed the increase of Si concentrations in the sediments as high as 10 g L^{-1} caused by the injection of a concentrated NaOH solution through sediments [6]. The maximum concentration of Si in experiments with water-saturated column experiments using NH_3-treated Hanford sediments was observed as 30mM [4]. So, the experimental test solutions were prepared in a wide range of Si concentration using 5 mM, 50 mM, 100 mM, 150 mM, 200 mM, and 250 mM to analyze different Si:Al ratios at varied between 0 mM and 100 mM bicarbonate concentrations. The Al concentration was kept constant at 5 mM. To evaluate the effect of calcium ions on the U(VI) removal, two concentrations of Ca were tested in the experiments, 5 mM and 10mM. The concentration of U(VI) in the experimental solutions was kept constant at 2 ppm. Experimental matrix is presented in TABLE 1.

TABLE 1. Experimental Matrix

Batch number	**HCO_3, mM**	**Si:Al molar ratio (Ca=5mM and Ca=10mM)**					
1	0	1	10	20	30	40	50
2	2.9	1	10	20	30	40	50
3	25	1	10	20	30	40	50
4	50	1	10	20	30	40	50
5	75	1	10	20	30	40	50
6	100	1	10	20	30	40	50

Stock solutions of 422.24 mM of Si ($Na_2SiO_3 \cdot 9H_20$), 50mM of aluminum ($Al(NO_3)_3 \cdot 9H_2O$), 400mM bicarbonate ($KHCO_3$), and 1250mM of Ca ($CaCl_2 \cdot 2H_2O$) were used as starting regents for solutions formulations. Uranyl nitrate hexahydrate was used as a source of U(VI).

For each bicarbonate concentration, six different test solutions were prepared at different Si:Al ratios by mixing measured volumes of the silicate and aluminum stock solutions. The mixture was then amended with the measured volume of appropriate bicarbonate stock solution and the pH of the resulting solution was adjusted to 8.0 by titrating with concentrated nitric acid. This pH was previously measured in the pore water composition [8]. The deionized water (DIW) was added to bring the final volume of the each test solution to 50mL. Then, NH_3 gas (5% NH_3 in 95% N_2) was injected into each solution through 20 μm pores of a metal gas sparger (Mott Corporation) until the pH of the solution reached a value of approximately 11. Three test samples, each with a volume of 5 mL, were extracted from each test solution and transferred to individual polyethylene 15mL tubes and then spiked with corresponding concentration of Ca and U(VI). Control samples amended with U(VI) at concentrations of 2 ppm were prepared in DIW to test for U(VI) losses from the solutions due to sorption to tube walls and caps. All control and experimental tubes were kept in an incubator/shaker at 100 rpm and at a temperature of 25°C. After two days, tubes were centrifuged for 5 minutes at 2000 rpm and supernatant solutions were analyzed for U(VI), Si, Al, and Ca. Si, Al, and Ca were measured using an inductively coupled plasma optical emission spectrometer (ICP-OES, OPTIMA 7300DV, Perkin-Elmer). Aqueous uranium U(VI) concentrations were analyzed via a Kinetic Phosphorescence Analyzer KPA-11 (Chemcheck Instruments, Richland, WA). For analysis with the KPA, an aliquot was extracted from the supernatant of each test sample and diluted with 1% nitric acid between 5 to 100 times. For analysis with the ICP-OES, an aliquot extracted from the supernatant of each test sample was diluted in conical polypropylene tubes between 100 to 200 times with DIW. For better accuracy, the concentration of elements was analyzed using different dilutions factors.

The predominant uranium species in the solutions were calculated via Visual MINTEQ equilibrium modeling software (v. 3.0, maintained by J.Gustafsson at KTH, Sweden), and updated with the Nuclear Energy Agency's thermodynamic database for uranium [2] and calcium-uranyl-carbonate complexes from [9]. The software calculated uranium speciation in the elements of interest and saturation indexes for solid phases.

RESULTS

Experimental results were evaluated based on the percent removal of the elements of interest: U(VI), Si, Al, Ca, and inorganic carbon (IC). Fig.1 – Fig.3 depict the percent removal of these elements in solutions where pH was increased up to 11 as a result of NH_3 gas injection.

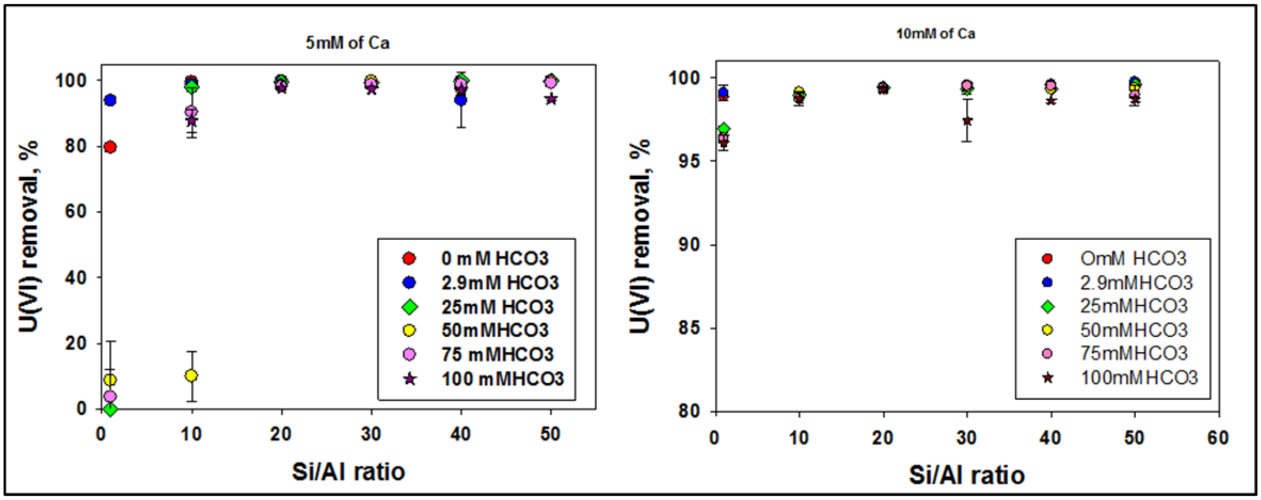

Fig.1. Removal of U(VI) in the solution mixture prepared with 5 mM and 10 mM of Ca.

The results indicated that the percentage of U(VI) removal was largely controlled by the Si/Al ratios and calcium concentrations. The percent of U(VI) removal increased as Si/Al ratios and calcium concentrations were increased. As noted from the results, the higher Ca concentration correlated with greater U(VI) removal, ranging between 96%-99%. This was especially notable at low Si/Al ratios between 1 and 10 (Fig. 1). Without Ca there was no observed reduction in the U(VI) concentration in the supernatant solutions at low Si/Al ratios [10]. Besides, starting from the Si/Al ratio 20 (Si ≥100mM), the removal of U(VI) yielded 98%-99%, which seemed to have overshadowed previous results without Ca ions introduced in the solution. Compare to samples without Ca, samples amended with Ca have not revealed significant changes in the percent removal of U(VI) in respect to increasing bicarbonate concentrations [10].

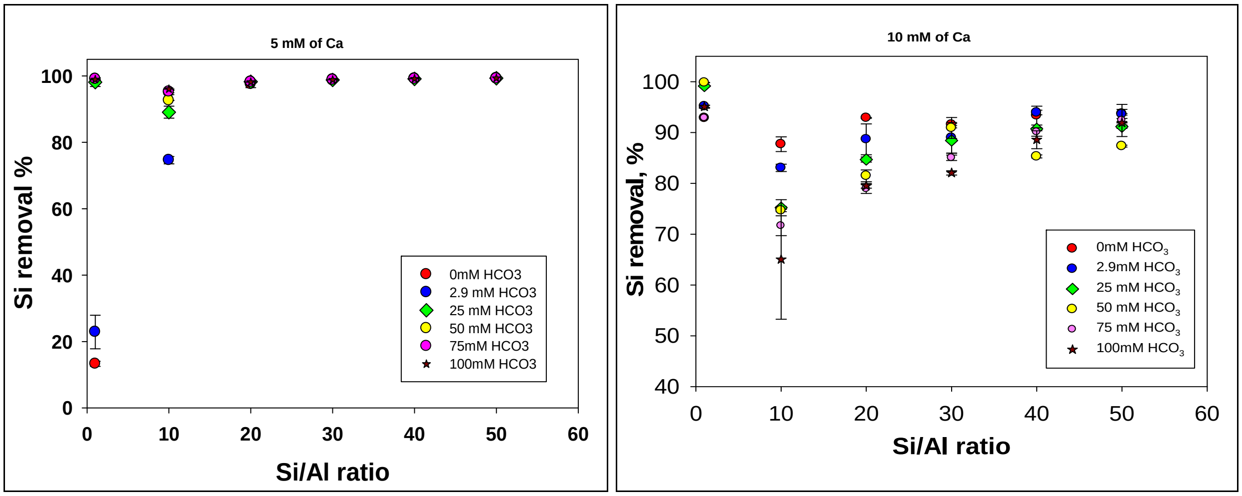

Fig. 2. Removal of Si in the solution mixture prepared with 5 mM of Ca and 10mM of Ca.

Similar observations were made for Si removal (Fig. 2). The results suggest that the percent removal of Si increases with an increase in Si concentration in solution and the increase in Ca concentration correlated with higher removal of Si from the supernatant of the solution mixtures at low Si/Al ratios. When the Ca concentration was increased up to 10 mM, the percentage of silica removal at Si:Al ratio 1, the lowest ratio investigated in this study, was increased to 93-99%. In all of the experiments, the removal of Si correlated with the removal of U(VI) from solutions. If the supernatant solutions showed a small decline in Si concentrations, the removal in U(VI) was diminutive or not observed.

Under alkaline conditions, $Al(OH)_4^-$ is the dominant species for Al. It concentration at Si/Al =1 showed some variability, but when the concentration of Si increased at Si/Al molar ratio ≥10, Al concentration dropped to almost undetectable level. Monomeric silica reacts with Al^{3+} ions following its precipitation due to a reaction between $Si(OH)_4$ and crystalline $Al(OH)_3$. When the silica concentration is below the solubility of amorphous silica in water, no polymerization occurs except when alumina is added. Iler (1979[11]) proposed that SiO_2 surfaces exposed to solutions containing aluminum formed aluminosilicate surface complexes by reaction with the hypothetical stoichiometry:

$$> SiOH + Al(OH)_3^{+} \leftrightarrow \; > SiOAl(OH)_2 + H^{+} \quad \text{[Eq.3]}$$

The formation of aluminosilicate chains upon mixing monosilicic acid and $Al(OH)_3$ acting as nuclei or “seeds” can accelerate Si polymerization reactions. The presence of aluminum results in an entire armored surface coating, which is extensive enough to reverse a net negative Si surface charge to positive [11,12].

According to speciation modeling, the dominant Ca species in the solution at the tested conditions are free Ca^{2+} ions, $CaHCO_3^+$, $CaCO_3$ with minor formation of $CaNH_3^{+2}$, $Ca(NH_3)_2^{+2}$ and Ca-U-CO_3. The speciation modeling hasn't predicted the formation of calcium silicate at this elevated pH condition and the removal of Ca^{2+} ion from the solution apparently is mostly due to the precipitation of calcium carbonate (Fig. 3).

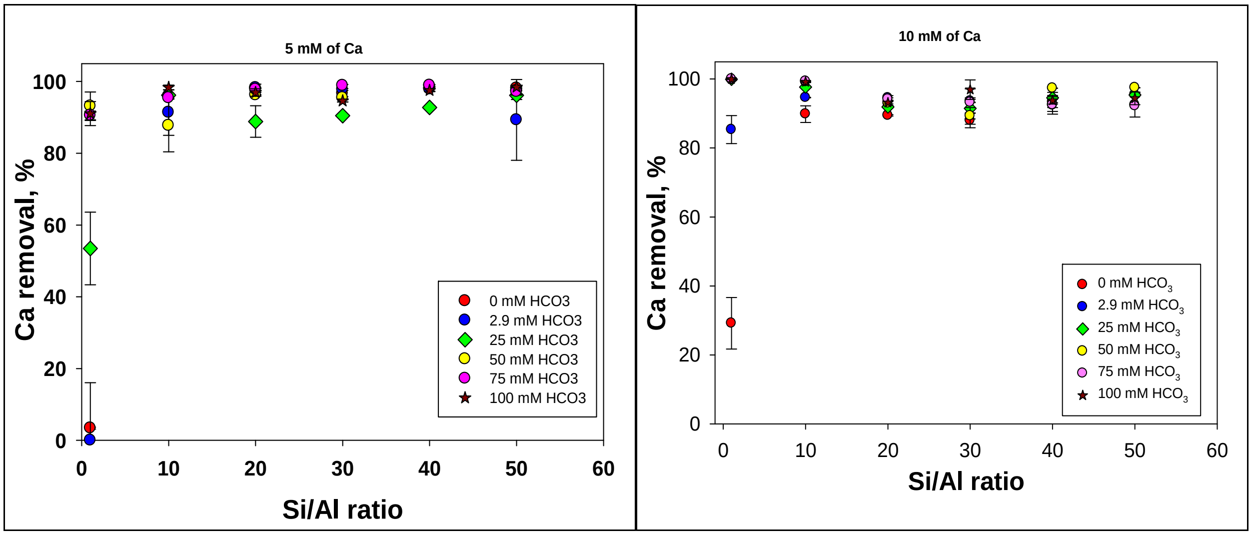

Fig. 3. Removal of Ca from the solution mixture prepared with 5 mM of Ca and 10mM of Ca.

The precipitation of calcium carbonate controls the removal of inorganic carbon from the aqueous solution. Speciation modeling suggested that calcium carbonate accounts for 19.1-68.1%, 14.1-20.5%, and 8.0-19.0% of the total bicarbonate concentrations present initially in the solution at the 3 mM, 25 mM and 50-100 mM range, respectively. However, experimental results showed that the removal of inorganic carbon is much higher reaching at some instances 80%. We hypothesized that the discrepancies between MINTEQ- predicted formation of $CaCO_3^{2-}$ and the experimental removal of inorganic carbon are coagulation and encapsulation within the silicate polymer that retained carbonate solids with polymerized silica gel. Precipitation of $CaCO_3$ and its encapsulation within Si sols cause changes in the carbonate system due to the decrease in the calcium carbonate saturation state. It is especially noticeable at higher Si and HCO_3^- concentrations in solution. In previous studies, silica uptake onto calcium carbonate was shown to increase in higher-ionic-strength solutions and higher silica aqueous concentration [13].

According to the speciation modeling predictions, at 0 mM HCO_3, U(VI) is present in the solution dominantly as $UO_2\,(OH)_3^-$. In the solutions amended with bicarbonate, $Ca_2UO_2(CO_3)_3$ and $CaUO_2(CO_3)_3^{-2}$ are the predominant species accounting for 30%- 84% of the total uranium species. Saturation indexes showed that potential U-bearing secondary phases as becquereline, gummite, rutherfordine, and schoepite are undersaturated at all conditions tested. However, speciation modeling predicted the formation of aragonite and calcite in addition to various aluminosilicate and aluminum hydroxide solid phases created out of elements present in the solution. These solid phases can serve as potential nuclei that trigger Si polymerization reactions. This leads to the co-precipitation of U solids (as U hydroxide and/or Ca-U-CO_3) within the amorphous structure of Si-Al-$CaCO_3$ precipitates.

CONCLUSIONS

Our results provided details on the effect of various Si/Al ratios and calcium concentrations on the removal of uranium from the synthetic solution mixture. From the experiments, it is evident that solutions with higher concentrations of Si and Ca tended to have greater removal efficiencies of U(VI) reaching up to 98-99%. In the presence of 5 mM and 10mM of Ca, the removal of U(VI) have overshadowed previously obtained results without Ca ions introduced in the solution. When the Ca concentration was increased up to 10 mM, the percentage of silica removal at Si:Al ratio 1, the lowest ratio investigated in this study, was increased to 93-99%. Higher Si removal in the presence of Ca^{2+} ions was probably due to silica coagulation by calcium ions leading to precipitation of those elements from the tested solutions [11]. However, the geochemical equilibrium modeling hasn't predicted the formation of calcium silicate species limiting Ca species only to $CaHCO_3^+$, $CaCO_3$, $CaNH_3^{+2}$, $Ca(NH_3)_2^{+2}$, and Ca-U-CO_3 complexes. Overall, the formation of precipitate always correlated with the removal of U(VI), Si, Al and Ca from the solution. If no precipitate formation was observed, there was no U removal from the supernatant solution. Visual Minteq modeling predicted that U(VI) present in solution dominantly as $Ca_2UO_2(CO_3)_3$ and $CaUO_2(CO_3)_3^{-2}$ and Ca-UO_2-CO_3 ternary complexes constitute up to 84% of uranyl species. The solid phase characterizations of uranium-bearing precipitates prepared with Ca are ongoing by means of X-ray diffraction and SEM/EDS techniques. These results further our understanding of uranium removal after the ammonia gas injection in the Hanford VZ.

ACKNOWLEDGEMENTS

Funding for this work was provided by the U.S. Department of Energy Office of Environmental Management under grant DE-EM0000598.

REFERENCES

1. Langmuir, D., 1978. Uranium solution–mineral equilibia at low temperatures with application to sedimentary ore deposits. Geochimica et Cosmochimica Acta 42, 547-569.
2. Guillaumont R., Fanghänel T., Fuger J., Grenthe I., Neck V., Palmer D.A., Rand M.H., 2003. Chemical Thermodynamics, OECD Nuclear Energy Agency vol. 5, Elsevier, 919 pp.
3. Denham, M and B. Looney, 2005. Gas: A Neglected Phase in Remediation of Metals and Radionuclides. Report WSRC-MS-2005-00589.Dong, W. and S.C. Brooks, 2006. Determination of the formation constants of ternary complexes of uranyl and carbonate with alkaline earth metals ($Mg^{2+,}$ Ca^{2+}, Sr^{2+}, and Ba^{2+}) using anion exchange method. Environ. Sci. Technol. 40(15):4689-4695. doi: 10.1021/es0606327
4. Szecsody JE, MJ Truex, L Zhong, TC Johnson, N Qafoku, MD Williams, WJ Greenwood, EL Wallin, JR Bargar, and DK Faurie. 2012. "Geochemical and Geophysical Changes during Ammonia Gas Treatment of Vadose Zone Sediments for Uranium Remediation." Vadose Zone Journal 11(4):, doi:10.2136/vzj2011.0158
5. Chou, L and R. Wollast, 1984. Study of the Weathering of Albite at Room Temperature and Pressure with a Fluidized Bed Reactor. Geochimica et Cosmochimica Acta 48, 2205-2217.

6. Szecsody, JE, MJ Truex, L Zhong, MD Williams, CT Resch, JP McKinley, 2010b. Remediation of Uranium in the Hanford Vadose Zone Using Gas-Transported Reactants: Laboratory-Scale Experiments. PNNL-18879. Contract DE-AC05-76RL01830.
7. Szecsody, J., M. Truex, L. Zhong, N. Qafoku, M. Williams, J. McKinley, et al. 2010a. Remediation of uranium in the Hanford vadose zone using ammonia gas: FY 2010 laboratory-scale experiments. PNNL-20004. Pac. Northw.Natl. Lab., Richland, WA.
8. Serne RJ, Lindberg MJ, Baum SR, Last GV, Clayton RE, Geiszler KN, Gee GW, LeGore VL, Brown CF, Schaef HT, Orr RD, Valenta MM, Lanigan DC, Kutnyakov IV, Vickerman TS, Lindenmeier CW, 2008. Characterization of Vadose Zone Sediment: Borehole 299-E33-45 Near BX-102 in the B-BX-BY Waste Management Area. PNNL 14083 Rev.1. Prepared for the U.S. Department of Energy.
9. Dong, W. and S. C. Brooks, 2006. Determination of the formation constants of ternary complexes of uranyl and carbonate with alkaline earth metals (Mg^{2+}, Ca^{2+}, Sr^{2+}, and Ba^{2+}) using anion exchange method. Environ. Sci. Technol. 40(15):4689-4695. doi: 10.1021/es0606327
10. Katsenovich, Y., Gonzalez, N., Moreno-Pastor, C., Lagos, L., 2012. The Effect of Si and Al Concentration Ratios on the Removal of U(VI) under Hanford Site 200 Area Conditions. In the proceeding of the Waste Management Conference, Feb 26 –March 2, 2012, Phoenix, AZ.
11. Iler, R.K., 1979. The chemistry of silica: solubility, polymerization, colloid and surface properties, and biochemistry. John Wiley and Sons, p.886.
12. Dove, P.M. and J.D. Rimstidt, 1994. Silica-Water Interactions, Reviews in Mineralogy Series: The Silica Polymorphs., Eds. P. Heaney, C. Prewitt and G. Gibbs, Volume 29, Mineralogical Society of America, pgs. 259-308.
13. Kitano, Y., Okumura, M. and Idogaki, M., 1979. Behavior of dissolved silica in parent solution at the formation of calcium carbonate. Geochem. J., 13: 253-260.